Studies on the Cell Cycle Lengthening of Epidermal Cells during Neurulation in Ascidian Embryos

Studies on the Cell Cycle Lengthening of Epidermal Cells during Neurulation in Ascidian Embryos

January 2014

Yosuke OGURA

Studies on the Cell Cycle Lengthening of Epidermal Cells during Neurulation in Ascidian Embryos

A Dissertation Submitted to

the Graduate School of Life and Environmental Sciences,

the University of Tsukuba

in Partial Fulfillment of the Requirements

for the Degree of Doctor of Philosophy in Science

(Doctoral Program in Biological Sciences)

January 2014

Yosuke OGURA

Table of Contents

Abbreviations

a.a.	amino acids
AP-2	activator protein 2
BCIP	5-Bromo-4-Chloro-3'-Indolylphosphatase p-Toluidine salt
cdc25	cell division cycle 25
Cdk1	cyclin dependent kinase 1
eCFP	enhanced cyan fluorescent protein
EF1α	elongation factor alpha
En	engrailed (A gene from *Drosophila*)
Epi1	epidermis specific gene 1
GSK3β	glycogen synthase kinase 3 beta
hGem(1/110)	human geminin (amino acid from 1 to 110)
hpf	hour post fertilization
IF	intermediate filament
MBT	mid-blastula transition
mAG	monomeric version of Azami Green (fluorescent protein)
mCherry	monomeric version of DsRed (fluorescent protein)
MD	mitotic domain
MO	morpholino oligonucleotide
mVenus	monomeric version of Venus-YFP (fluorescent protein)
NBT	nitro-blue tetrazolium chloride
PCNA	proliferating cell nuclear antigen
PH3	phosopho-histone H3
WISH	whole mount *in situ* hybridization

1. Abstract

The central nervous system in chordates is formed through the morphogenetic processes during neurulation. Neurulation is initiated by the bending of neural plate and completed by the fusion of neural folds at the midline. Cell type specific cell cycle regulation in neural and non-neural tissues contributes for neurulation. In this study, I have analyzed the cell cycle regulation of epidermal cells during neurulation in a chordate ascidian *Ciona intestinalis*. Epidermal cells undergo 11 times of mitoses from the 1-cell stage until the tailbud stage. At first, I discovered that the fusion of neural folds occurs during the last cell cycle (11th cell cycle) of epidermal cells. The interphase length of epidermal cells during neurulation is twice longer than the previous cell cycles during gastrulation. Through genetic and pharmacological experiments, I show that this interphase lengthening facilitates the cell movement of epidermal cells required for neural fold fusion. Secondly, to reveal cell type specific control of cell cycle progression in the epidermal cells, I undertook *cis*-regulatory analysis of *cdc25* which promotes cell cycle progression of epidermal cells. Specifically, I discovered the binding sites of transcription factors AP-2 and GATA in the epidermal enhancer of *cdc25*. The roles of AP-2 and GATA have been implicated at the interface of proliferation/differentiation during mammalian embryogenesis and oncogenesis. Through genetic experiments and fluorescent time-lapse imaging, I show that AP-2 and GATA activates *cdc25* transcription, thereby regulating the interphase length of epidermal cells. I further show that down-regulation of *AP-2*, which occurs at the onset of neurulation in normal embryogenesis is required for subsequent *cdc25* down-regulation. This study identified the epidermis specific program for transcriptional regulation of *cdc25* that is essential for the cell cycle regulation during neurulation in *Ciona*.

2. Introduction

Neurulation is a morphogenetic process to form the dorsal hollowed neural tube, a precursor of brain and spinal cord in chordates. At least three types of morphogenetic processes are observed during vertebrate neurulaion; bending of neural plate, migration of neural folds and fusion of neural folds (Copp et al., 2003). Proliferation of neural and non-neural cells supports the morphogenetic processes during neurulation. Therefore, cell cycle progression of neural and non-neural fated cells must be carefully regulated during neurulation (Copp et al., 1988; Copp et al., 2003). For example, proliferation is reduced in the bending region of the neural plate, which is thought to be relevant to the bending of neural plate (Smith and Schoenwolf, 1988). The morphogenetic processes during neurulation require not only intrinsic force within neural plate but also extrinsic forces from neighboring tissues. Proliferation of mesenchyme activated by transcription factor Twist (Chen and Behringer, 1995) and hindgut endoderm proliferation promoted by Grainyhead-like3 (Gustavsson et al., 2007) are required for proper morphogenetic processes during neurulation. The fusion of neural folds is regulated by the transcription factor Activator protein 2 (AP-2) (Schorle et al., 1996). AP-2 regulates cell fate determination and cell proliferation of epidermis. It is thought that the activity of AP-2 have to be regulated during neurulation (Nottoli et al., 1998). Thus, cell proliferation coupled with cell fate determination in several tissues plays essential role for proper neurulation. However, role of cell cycle regulation and mechanisms of cell type specific cell cycle regulation during neurulation are not fully elucidated in vertebrates, possibly owing to its complexity.

Cell cycle progression during animal embryogenesis is controlled by the activities of Cyclin-dependent kinases (Cdks). Cdk-cyclin complexes are kept inactive

by binding to a Cdk kinase inhibitor (CKI) and/or through inhibitory phosphorylation by the Wee1 and Myt1 kinases. The activation of Cdk-Cyclin complexes is triggered when CKI is released and/or the inhibitory phosphate groups are removed through the action of Cdc25 phosphatase family members (Malumbres and Barbacid, 2009; Budirahardja and Gönczy, 2009). In *Drosophila* embryogenesis, cell cycle progression after the gastrulation is triggered by *cdc25*/*string* transcription (Edgar and O'Farrell, 1990). The cell type specific *string* gene expression is regulated by transcription factors involved in the cell fate determination. They act through the *cis*-regulatory elements of *string* (Lehman et al., 1999). Cell type specific transcription of *cdc25* has been suggested to play a role in the control of embryonic cell cycle in vertebrate model organisms (Wickramasinghe, 1995; Nogare et al., 2007; Ueno et al., 2008).

The embryo of chordate ascidian *Ciona intestinalis* is an excellent model to investigate the cell cycle regulation during neurulation. The *Ciona* embryo undergos neurulation closely related to the primary neurulation in vertebrates (Nicol and Meinertzhagen, 1988; Lowery and Sive, 2004). The neurula stage embryo is composed of only 500 cells. Taking advantage of a small, fixed cell number and simple tissue architecture, the morphogenesis and the cell lineage during neurulation have been described at a single cell level (Nicol and Meinertzagen, 1988; Cole and Meinertzagen, 2004). In this study I used the *Ciona* embryo as a model to investigate the cell cycle regulation during neurulation. In particular, I have analyzed cell cycle regulation of epidermal cells during neurulation by performing live imaging of cell cycle progression and morphogenetic movement of epidermal cells. The epidermal cells of the *Ciona* embryo undergo eleven times of mitosis from the 1-cell stage until the tailbud stage. I found that the interphase is lengthened nearly two fold at the 11th cell cycle when the

epidermal cells perform characteristic F-actin mediated cell movement required for neural fold fusion. By performing genetic experiment and live imaging, I show that this cell cycle lengthening is necessary for the competition of neurulation. I also discovered that two cell type specific transcription factors Ci-AP2L2 and Ci-GATA-b regulates the transcription of *Ci-cdc25* in the epidermal cells through its *cis*-regulatory element. I further show that down-regulation of *AP-2*, which occurs at the onset of neurulation in normal embryogenesis is required for subsequent *Ci-cdc25* down-regulation. Thus, these studies on cell cycle regulation of the epidermal cells revealed the coupling of cell cycle and cell fate determination in *Ciona*. The coupling of cell cycle and cell fate determination might be crucial for morphogenetic processes during neurulation in *Ciona*.

3. Materials and Methods

3.1 Embryo culture and manipulation

Wild-type *Ciona intestinalis* was collected from or cultivated at Onagawa(Miyagi), Maizuru (Kyoto), Mukaishima (Hiroshima) and Usa (Kochi). In blastomere isolation experiments, cleaving embryos were transferred into Ca^{2+} and Mg^{2+} free artificial sea water and dissected at the 8-cell stage using glass needle. DNA electroporation was carried out using a GenePulser Xcell™ (Bio-Rad) as described previously (Corbo et al., 1997). The parameters were set as follows; time constant; 20 ms voltage; 50 V. The amount of DNA introduced was 60 μg for each vector.

3.2 Constructs

A *gap43-egfp* fusion was amplified by polymerase chain reaction (PCR) using

pSP72-pFOG::B1-GAP43-GFP-B2 (Roure et al.,2007) as a template and inserted into pSP-eGFP to create pSPGAP43G. *egfp* was replaced by *ecfp* to create pSPGAP43C. A *Ci-Epi1* promoter was inserted into pSPGAP43C to create pSPCiEpi1GAP43C. A CAAX box (Fukano et al., 2007) was subcloned into the C terminus of the *Kaede* open reading frame (ORF) of pSPKaede (Hozumi et al., 2010) to create pSP-KCAAX. A *Ci-Epi1* promoter was inserted into pSPKCAAX to create pSPCiEpi1KCAAX. The *egfp* cDNA of pSP-eGFP was replaced with cDNA of *Ci-cdc25* to create pSPCicdc25. A *Ci-Epi1* promoter was inserted into pSPCicdc25 to create pSPCiEpi1Cicdc25. *CiEpi1-gap43-ecfp* or *CiEpi1-Kaede-CAAX* cassettes were subcloned into pSPCiEpi1Cicdc25 to create pSPCiEpi1Cicdc25CiEpi1GAP43C and pSPCiEpi1Cicdc25CiEpi1KCAAX. A Histone 2B ORF (Roure et al., 2007) fused with mCherry-RFP at the N-terminus was inserted into pSP-eGFP to create pSPH2BmCherry. The *Ci-EpiI* promoter was inserted into the multi-cloning site of pSPH2BmCherry to create pSPCiEpiIH2BmCherry.

The cDNA for mAG-hGem(1/110), mVenus-hGem(1/110) (Sakaue-Sawano et al., 2008). *Ci-cdc25*, *Ci-AP2-like2* (*Ci-AP2L2*) were cloned into pHTB (Akanuma et al., 2000). The cDNA for *Ci-GATA-b* was cloned into pBSRN3 (Lemaire et al., 1995). cDNA encoding En-GATA-a, which consists of the transcription repressor domain from *Drosophila* Engrailed (amino acids 298) fused to the N terminus of Ci-GATAa DNA binding domain (amino acids 303-422) were made by PCR and cloned into the pBSRN3. This construct was previously reported to act in dominant negative fashion on GATA-a (Bertrand et al., 2003). Similarly, I cloned En-Ci-AP2L2 (amino acid 334-535 of Ci-AP2L2) into the pBSRN3. The cDNA of *mVenus*-YFP (Nagai et al., 2002) and *Ci-PCNA* was cloned into the *Not*I/*Kpn*I site and *Kpn*I /*Eco*RI site of pSPeGFP

(Sasakura et al., 2003) respectively. The resultant construct, pSPmVenusPCNA was cut with *Not*I and *Eco*RI and cloned into *Not*I/*Eco*RI site of pHTB to create pHTBmVenusPCNA. mRNA was synthesized with the Megascript T3 (Ambion), cap structure analog (New England Biolabs), and poly(A) tailing kit (Ambion).

A *cis*-regulatory region upstream of the first nucleotide to the initiator ATG of *Ci-cdc25* was cloned into the *Bam*HI site of pSPKaede (Hozumi et al., 2010). The epidermal enhancer of *Ci-cdc25* (1983 bp - 2110 bp upstream from the ATG) was placed upstream of *Ci-fkh* basal promoter which includes the 148 bp upstream from the ATG. (Hozumi et al., 2013). The upstream regulatory sequence was analyzed by phylogenetic foot-printing using Vista (http://pipeline.lbl.gov) (Frazer et al., 2004). Deletion or mutation constructs within the putative binding sites of transcription factors were obtained by recombination PCR. GATA sites were mutated to AATA. AP-2 sites were mutated to GTC.

3.3 Immunostaining and phalloidin staining

mVenus-hGem(1/110) was immunostained with anti-GFP antibody (1:1000; Nacalai Tesque) and Alexa-488-conjugated anti-rabbit antibody (Invitrogen) for observation of EdU incorporation in Fucci-expressing embryos. To detect Phospho-histone H3 (PH3), pSPCiEpiIH2BmCherry was introduced into embryos, which were fixed at 7.75 hpf. PH3 was stained with anti-PH3 Ser10 antibody (1:100) (Tarallo and Sordino, 2004) and Alexa-488 conjugated anti-rabbit antibody. Embryos were stained with Alexa-488-conjugated phalloidin (Invitrogen) to detect F-actin.

3.4 Morpholino-oligonucleotide mediated knockdown of genes

Three morpholino oligonucleotides (MOs), *Ci-cdc25* MO (5'-CGGCTGAAATCGGAAACAAATGTTA-3'); *Ci-AP2L2* MO (5'-TGTATCTGGAATAATAGCAAGTGTT-3'); *Ci-GATA-b* MO (5'-ATTGTTACGTCATAATCACCTGTGC-3') were designed to bind to exon-intron junctions of the corresponding genes. The ability of these two MOs to disrupt splicing was assessed by reverse-transcription (RT)-PCR using the cDNA made from the RNA extracted from the embryos at the gastrula stage or the tailbud stage. The details are shown in Fig.14. *Ci-SoxB1* MO (5'- TAACATGAAGTCGTTCTGAGATGGC-3') was designed to bind to the initiation codon of *Ci-SoxB1* mRNA. The translation inhibition ability of the MO was assessed by examining expression of *Kaede* reporter protein from the construct prepared by inserting a genomic DNA fragment of 4.1 kbp upstream the *Ci-SoxB1* gene (Fig. 15). The MOs were injected at a pipette concentration of 0.125 mM (*Ci-cdc25* MO), 1 mM (*Ci-AP2L2* MO), 0.5 mM (*Ci-GATA-b* MO) and 0.5 mM (*Ci-SoxB1* MO), respectively.

3.5 Real time quantitative PCR

Total RNA was extracted from embryos using Isogen (Nippon Gene). Genomic DNA was digested with DNaseI (Takara Bio). Reverse transcription was performed with Superscript III reverse transcriptase (Invitrogen) and Oligo(dT) primers. Realtime (RT) quantitative PCR was carried out with SYBR Premix Ex Taq II (Takara Bio) and a Thermal Cycler Dice Real Time System TP800 following the manufacturer's instructions. *Ci-EF1α* was used as a normalizer gene. The PCR primers for *Ci-EF1α* were 5'- CATGTCACGGACAGCGAAACG-3' and 5'-

CAATGTGTGTTGAGGCATTCCAAG -3', for *Ci-cdc25* were
5'-CGAGTATGCACTCTATCCACTG-3' and
5'-CAGTCAATCACCTCGAAACGAC-3', for *Ci-GATA-b* were
5'-GAGTATTTCATCGCATCGTC-3' and 5'-TTCCTCTGTCTTCACCAATG-3'.
for *Ci-AP2L2* were 5'-ACGACCTCGAAGGTTTCGTTC-3'and
5'-ATCGGTGACAACATGTCAGCTG-3'.

3.6 Whole-mount *in situ* hybridization

Whole-mount *in situ* hybridization (WISH) was performed basically according to the method described by Yasuo et al. (1993). The signals were visualized with NBT-BCIP. Digoxigenin(Dig)-labeled RNA probes for *in situ* hybridization for *Ci-IF-C*, *Ci-IF-D*, *Ci-Epi1* and *Ci-AP2L2* were synthesized using the Gateway-compatible open reading frame (ORF) clones as templates. Gateway is the technology of the Invitrogen and was applied to *Ciona* cDNA library in Roure et al., 2007. *Ci-cdc25* cDNA and *Ci-GATA-b* cDNA were cloned into pBS-SKII+, and Dig-labeled RNA probe was synthesized using the vector as the template. 1-azekenpaullone was dissolved in dimethyl sulfoxide (DMSO). Embryos were treated with 1-azakenpaullone containing seawater, and used at the final concentration of 10 μM.

3.7 Time-lapse imaging using wide-field microscopy

The embryos were reared at 18°C until imaging. Time-lapse imaging was performed using the AxioImager Z1 wide-field fluorescent microscope system (Carl Zeiss) and the 10x water-emersion objective. Imaging was performed in a room maintained at 20°C. I found no significant deviation from the developmental table (Hotta et al., 2007) defined

at 18°C until 8.5 hours post fertilization (hpf). pSPCiEpi1GAP43C and pSPCiEpi1CiCdc25CiEpi1GAP43C (linearized with *Xho*I) were microinjected into unfertilized eggs together with mVenus-hGem(1/110) mRNA. At 6.0 hpf, the embryos were mounted on a glass-based dish, and time-lapse imaging was performed. The recording interval was 5 minutes. In the aphidicolin administration experiment, imaging was halted at 6 hours 55 minutes, aphidicolin was added at the concentration of 2 μg/ml, and imaging was restarted from 7.0 hpf.

3.8 Time-lapse imaging using confocal laser scanning microscopy

The embryos were injected with mRNA encoding mVenus-PCNA at the 1-cell stage followed by injection of mRNA encoding *Ci-cdc25* or MOs against *Ci-GATA-b* or *Ci-AP2L2* into a single blastomere of the 2-cell stage embryos. The embryos were mounted on a glass-base dish (Iwaki) and time-lapse 3D imaging was performed on inverted confocal scanning microscope LSM700 (Carl Zeiss) using a ×60 oil-emersion objective or ×10 objective. Two laser lines, 488 nm and 555 nm were used. The stage was cooled down at 17 - 18 °C until using F25-EH refrigerated/heating circulator (Julabo). The imaging was started at 4.5 hpf, just before the 8th mitosis of epidermal cells has started. The recording interval was 2 minutes. Image processing and analysis were performed using ImageJ software (http://rsbweb.nih.gov/ij/).

4. Results

4.1 Mitotic timing of epidermal cells during neurulation

To observe the spatiotemporal regulation of mitosis in the epidermis, I performed time-lapse imaging using a fluorescent probe mAG-hGem(1/110) which was designed

to label the cells in S/G2/M phase (Sakaue-Sawano et al., 2008). hGem(1/110) contains nuclear localization signal. *In vitro*-synthesized mRNA of mAG-hGem(1/110) was introduced into unfertilized egg by microinjection and observation was begun after fertilization. As expected, I observed nuclear localization of mAG-hGem(1/110) fluorescence during interphase and its dispersal at the prometaphase entry. The fluorescence of mAG-hGem(1/110) was observed as early as the beginning of the 9th cell cycle (Fig. 1A). The 9th mitosis occurred at 5.5 - 6.0 hpf. The b-line (posterior) epidermal cells entered mitosis approximately 5 min faster than a-line cells, as was described previously (Nishida, 2005). The 10th mitosis occurred at 6.5-7.0 hpf (Fig. 1B). I found that the timing of this mitosis differed along the anterior-posterior (A-P) axis of the embryo. Posterior cells tended to enter mitosis earlier than anterior cells. The 11th mitosis occurred around 8.0 - 9.0 hpf (Fig. 1C). At the time of the 11th mitosis, epidermal cells can be subdivided into four groups of cells that share the timing of mitosis. Such subdivision of cells according to the mitotic timing is called mitotic domain (Foe and Odell, 1989). In this study, I subdivided the epidermal cells into four groups according to their mitotic timing (Fig. 1D); cells around the ventral midline (MD1) and dorsal midline (MD2) and cells on the trunk lateral side (MD3a) and tail lateral side (MD3b). The 11th mitosis started in the order of MD1, MD2 and MD3. In MD1, MD2 and MD3a, posterior cells started mitosis earlier, and the mitotic wave moved toward the anterior. Cells at MD3b showed a different pattern: mitosis started from both the anterior and posterior side, and cells at the middle part performed mitosis later.

4.2 Fusion of left and right neural folds occurs at the eleventh interphase of the epidermal cell cycle

In addition to spatial pattern of mitoses, I noticed that the intervals between the prometaphases of the 10th and 11th mitosis were on average of 36 - 47 min longer than those between the 9th and 10th mitosis for cells of each mitotic domain (Fig. 1E; Table 1). A plausible role of the interphase lengthening of epidermal cells is to make the time for morphogenetic cell movement. I performed time-lapse imaging to analyze the morphogenetic cell behaviors of epidermal cells during the 11th interphase. Cell shape was visualized by expressing membrane-bound fluorescent proteins in the epidermal cells. Significantly, I found that the migration of epidermal cells and the fusion of left and right neural folds at the dorsal midline occur at the 11th interphase. Epidermal cells that had finished the 10th mitosis (i.e. at the interphase) were polygonal shaped (Fig. 2A, 0 min). At the onset of neural tube closure, epidermal cells at the posterior midline become elongated toward a focus at the dorsal midline (Fig. 2A, arrowheads). These epidermal cells made contact at the focus, which then became the origin of zippering. The left and right epidermal cells moved toward the dorsal midline, changed their shape to fill the gap and aligned tightly along the midline to close the furrow (Fig. 2A, 55 min). I also observed the formation of filopodia during the cell movement (Fig. 2C). The movement and alignment of midline epidermal cells were transmitted toward the anterior, and the midline was closed as if zipped (Fig. 2A, 80 min).

I found that F-actin fiber is accumulated at the leading edge of the epidermal cells during zippering (Fig. 2D, Control). Contraction of F-actin fiber accumulated at the leading edge of migrating cells, which is regulated by Rho/ROCK signaling is important for cell migration in animal cells (Raftopoulou and Hall, 2004). I found that

the F-actin accumulation and concomitant elongation of epidermal cells was inhibited by treating embryos with Y-27632 (Fig. 2D), an inhibitor of Rho-kinase (ROCK) (Uehata et al., 1997). This result suggests that the elongation of epidermal cells is activated by Rho/ROCK signaling. Inhibition of Rho/ROCK signaling also resulted in the failure of neural tube closure (Fig. 2D). After zippering, the epidermal cells performed the 11th mitosis (Fig. 2A, t = 170). Epidermal cells of all mitotic domains tended to divide parallel to the A-P axis (Fig. 2A, 170 min and Fig. 2B). When *Ci-cdc25* was overexpressed, the mitoses of epidermal cells still occurred parallel to the A-P axis (Fig. 2B). During neural tube closure, the tail started elongating toward the posterior end of the embryo (Fig. 2A).

4.3 *Ci-cdc25* regulates the interphase length of epidermal cells

As shown in the previous section, cell movement of epidermal cells during neurulation takes place during the 11th cell cycle. The length of interphase at the 11th epidermal cell cycle is about two fold longer than the interphase at the 10th epidermal cell cycle.
The *Ciona* genome encode a single *cdc25* orthologous gene (Kawashima et al., 2003), which I call *Ci-cdc25* in this study. *In situ* hybridization analysis of *Ci-cdc25* expression showed that *Ci-cdc25* expression is strong during gastrula stage (Fig. 3A, 5.0-6.0hpf) but is disappeared from the epidermis at the onset of neurulation when epidermal cells perform10th mitosis (Fig. 3A, 6.5 - 7.0hpf). Since epidermis is autonomously specified in *Ciona*, isolated blastomeres adopt epidermal fate and perform normal number of cleavages even the precursor blastomeres were isolated as early as 8-cell stage (Hudson and Lemaire, 2001, Yamada and Nishida, 1999). The precursor blastomeres of ectodermal cells (a4.2 and b4.2 pairs) were isolated at the 8-cell stage and cultured until

the time when control embryos undergo gastrulation and neurulation. Then, the amount of *Ci-cdc25* mRNA at 5.0 hpf, 6.0 hpf and 7.0 hpf was quantified (Fig. 3B). I found that the relative amount of *Ci-cdc25* mRNA at the neurula stage (7.0 hpf and 8.0 phf) was about one-third of the mRNA level at the gastrula stage (5.0 hpf) in the epidermal lineages. These results suggest that the expression of C*i-cdc25* in the epidermis is down-regulated at the onset of neurulation.

To examine whether zygotic expression of *Ci-cdc25* is involved in the regulation of the cell cycle length of epidermal cells, I disrupted the splicing of *Ci-cdc25* using antisense morpholino oligonucleotide (MO). In the embryos injected with *Ci-cdc25* MO, the splicing of *cdc25* mRNA was disrupted, resulting in the abnormal transcript lacking the sequence encoding catalytic motif of *Ci-cdc25* (Figs. 14A, B). Then I performed live imaging of cell cycle progression. I injected the embryos with the mRNA encoding mVenus-PCNA. The PCNA protein is a central component of the replication machinery localizes at the nuclei during interphase and is dispersed at the onset of pro-metaphase due to nuclear envelope breakdown (Leonhardt et al., 2000). I examined the effect injecting *Ci-cdc25* MO on the length of interphase. *Ci-cdc25* MO was micro-injected into a single blastomere at the 2-cell stage and the effect of MO injection on the cell cycle progression was evaluated using the un-injected side as an internal control. In the side injected with *Ci-cdc25* MO, the average length of the 10th interphase was longer up to 14.4 min (20.5%) compared to the control side not injected with *Ci-cdc25* MO. Similarly, the average length of the 11th interphase was longer up to 23.3 min (20.5%) in the side injected with *Ci-cdc25* MO compared to the control side (Fig. 3C). In contrast, the average length of the 10th interphase was shorter up to 11 min (18.6%) in the side injected with *Ci-cdc25* mRNA compared to the control

side. I also found that the average length of the 11th interphase was shorter up to 27.9 min (34%) in the side injected with *Ci-cdc25* mRNA compared to the control side (Fig. 3D). These results suggest that *Ci-cdc25* regulates the interphase length of epidermal cells. I also examined the effect of injecting *Ci-cdc25* MO or *Ci-cdc25* mRNA on the M-phase length, but I found no apparent difference in the M-phase length of epidermal cells (Figs. 20A, B).

To analyze the cell cycle phases shortened by *Ci-cdc25*, I also performed high resolution imaging of mVenus-PCNA fluorescence using ×60 oil emersion lens. Characteristic foci of mVenus-PCNA were observed in the nucleus during the interphase progression (Figs. 3E and 16). These foci might reflect mass of active replication forks at the closing minute of S-phase (late S-phase) as observed in other animals (Leonhardt et al., 2000; Philipova et al., 2005; McCleland et al., 2009; Leung et al., 2011). Even though I couldn't discriminate G1 phase and S-phase with this method, I could examine the effect of *Ci-cdc25* overexpression on the late S-phase timing and G2 phase length. I compared interphase progression in the cells injected with *Ci-cdc25* mRNA to that of un-injected cells. An example is shown in the Fig. 3E. At the 10th cell cycle, in the control cell, characteristic foci were observed at 32 min after the completion of 9th mitosis, while in the cell injected with *Ci-cdc25* mRNA, characteristic foci were observed as early as 18 min after the completion of 9th mitosis. This result indicates that interphase shortening observed in *Ci-cdc25* overexpressed cell is caused by the acceleration S-phase progression and shortening of G2 phase. Similar effect was observed in the 10th and 11th epidermal cell cycle (Fig. 15), suggesting that *Ci-cdc25* shortens the interphase by accelerating S-phase progression and shortening of G2 phase.

4.4 Shortening of the eleventh interphase of epidermal cells by *Ci-cdc25* overexpression disrupts neurulation

The above results suggest that down-regulation of *Ci-cdc25* might play an important role in the interphase lengthening of epidermal cells. I tried to reveal the role of interphase lengthening of the epidermal cell cycle in the morphogenetic processes during neurulation. I analyzed the cell cycle and morphogenetic movement of epidermal cells by performing dual color fluorescence time-lapse imaging using mVenus-hGem(1/110) and membrane-bound fluorescent protein. mVenus-hGem(1/110) can be used in a similar way as mAG-hGem(1/110) (Sakaue-Sawano et al., 2008). The fluorescence of mVenus-hGem(1/110) localized at the nuclei in the interphase and is dispersed at the M-phase. The expression of membrane-bound fluorescent protein was driven by the promoter of an epidermis specific gene *Ci-Epi1* (Chiba et al., 1998). As a control experiments, *in vitro*-synthesized mRNA of mVenus-hGem(1/110) and the plasmid construct encoding membrane-bound fluorescent protein was introduced into unfertilized egg by microinjection and observation was begun after fertilization. I confirmed that migration of epidermal cells and fusion of left and right neural folds was started after most of the epidermal cells finished 10th mitosis. Then, the 11th mitosis was observed only after the left and right neural folds meet at the dorsal midline (Fig. 4A). In the other words, the closure of epidermis took place at the 11th interphase.

Next, I examined the effect of overexpressing *Ci-cdc25* in the epidermis. *Ci-Epi1* promoter shows activity after the neurula stage and can be used to overexpress *Ci-cdc25* specifically after the neurula stage. In the embryos overexpressed *Ci-cdc25*, the 10th mitosis occurred on the normal timing. However, the 11th mitosis was initiated apparently earlier in these embryos. The timing of 11th mitosis was on average of 40

min faster than the controls (Fig. 4B). Precocious 11th mitosis of epidermal cells in the *Ci-cdc25*-overexpressed embryos was confirmed by immunostaining of phospho-histone H3 (PH3), a marker of cells during mitosis, at 7.75 hpf (Figs. 5A, B). These *Ci-cdc25*-overexpressed embryos failed to close the neural tube (80%, n = 25; Table 2). Forty percent of them showed a severe phenotype: they did not show neural tube closure in either the tail or trunk regions (Figs. 4B and 6B; Table 2). In these embryos, the epidermal cells underwent the 11th mitosis before the initiation of closure. Formation of a clear zippering origin was not observed at the posterior end of the embryos, and movement of the epidermal cells toward the midline did not occur (Fig. 6B and 7A). Forty percent of the embryos (Table 2) showed a milder phenotype: epidermal cells completed neural tube closure at the tail region but not at the trunk region (Fig. 6C; Table 2). The remaining 20% of the embryos completed neural tube closure (n=25; Table 2). In these embryos the 11th mitosis took place just after the closure, although the timing of mitosis was earlier than in the wild-type controls (Fig. 6D). These results suggest that the 11th mitosis of epidermal cells must take place after neural tube closure for proper morphogenetic movement to occur.

4.5 Interphase lengthening at the eleventh epidermal cell cycle is required for the morphogenetic processes during neurulation

If the failure in neural tube closure observed in *Ci-cdc25* overexpressed embryos results from the precocious 11th mitosis of epidermal cells, defects observed in neural tube closure should be rescued by arresting the epidermal cell cycle at the 11th interphase. To arrest cell cycle in the interphase, I treated embryos with aphidicolin, an inhibitor of DNA replication (Ikegami et al., 1978), between the 10th and 11th mitoses of the

epidermal cells and observed its effect on neural tube closure. When control embryos were treated with aphidicolin just after the 10th mitosis and before the 11th mitosis, neural tube closure at the tail region occurred as in the normal embryos (86%, n = 21). The trunk neural plate did not completely close in the aphidicolin-treated embryos. This could have been because cell-cycle progression of the trunk neural plate cells was also affected by aphidicolin. Thus, aphidicolin-treated embryos showed delayed or no 11th mitosis of epidermal cells, suggesting that aphidicolin effectively suppressed progression through the S phase of the 11th cell cycle.

Next, by using aphidicolin, I performed a rescue experiment of the overexpression phenotype of *Ci-cdc25* by arresting cells at the S phase. I noted the occurrence of neural tube closure at the tail (Fig. 7B). The fluorescent cross section of the embryos also confirmed the formation of normal organization of the neural tube in the tail region (Fig. 7C). As a result, the *Ci-cdc25*-overexpressed and aphidicolin-treated embryos showed neural tube closure at the tail much more frequently than did *Ci-cdc25*-overexpressed control embryos (Fig. 7B and Table 3). I also noticed that the accumulation of F-actin at the leading edge of epidermal cells was recovered in these *Ci-cdc25* overexpressed and aphidicolin-treated embryos (Fig. 2D). These results suggest that the precocious 11th mitosis caused by *Ci-cdc25* overexpression resulted in the failure in neural tube closure by interfering with the F-actin mediated cell movement of epidermal cells. The data also supports the idea that the interphase lengthening of epidermal cells at the 11th cell cycle is required for neural tube closure by facilitating the cell movement of epidermal cells.

4.6 Isolation of *cis*-regulatory element responsible for the epidermal expression of *Ci-cdc25*

Because *Ci-cdc25* shows clear zygotic expression during early embryogenesis (Figs. 3A and 19) and the disruption of *Ci-cdc25* splicing resulted in the lengthening of interphase of the epidermal cells (Figs. 3C and 14), transcriptional regulation of *Ci-cdc25* might play important role in the regulation of interphase length of the epidermal cells. To identify the mechanism of *Ci-cdc25* transcription, I investigated the *cis*-element of *Ci-cdc25* responsible for its epidermal expression. I performed deletion analysis of the upstream sequence of *Ci-cdc25* coding region. The results were summarized in the Fig. 8A. A genomic sequence 4976 bp upstream of the initiator ATG was placed upstream of a *Kaede* reporter gene to generate *pcdc25*(4976 bp)-*Kaede*. Reporter activity was examined by *in situ* hybridization using the probe against *Kaede* mRNA. In the embryos expressing the construct *pcdc25*(4976 bp)-*Kaede*, *Kaede* mRNA was detected in the entire epidermis from the gastrula stage until the tailbud stage. Transcriptional down-regulation of *Kaede* during neurulation was not observed, suggesting that *Kaede* expression does not recapitulates the endogenous expression of *Ci-cdc25*. This is probably because the large amount of mRNA transcribed from electroporated plasmids could not be fully degraded at the same extent to the endogenous *Ci-cdc25* mRNA. I obtained similar results using the constructs *pcdc25*(2295 bp)-*Kaede* and *pcdc25*(2109 bp)-*Kaede*.

Next, I examined the *Kaede* mRNA expression in the embryos expressing *pcdc25*(2010 bp)-*Kaede*. This construct showed weaker *Kaede* expression in the epidermis compared to *pcdc25*(2109 bp)-*Kaede*. In contrast, *pcdc25*(1983 bp)-*Kaede* showed almost no detectable signal in the epidermis, suggesting that the sequence

between upstream 2010 bp and 1983 bp is required for the reporter expression in the epidermis. Then, I tested the activity of upstream 2295 bp construct that was deleted with the sequence between upstream 1988 bp and 2110 bp (Figs. 8B and C). This construct also showed almost no detectable signal in the epidermis suggesting that the sequence between upstream 1988 bp and 2110 bp is responsible for the epidermal expression. To test whether this sequence has enhancer activity, I cloned the sequence between 1988 bp and 2110 bp upstream of basal promoter of *Ci-forkhead*. The construct showed Kaede reporter protein expression in the epidermis (Fig. 8D), suggesting that the region contains the element sufficient for driving gene expression in the epidermis. Hereafter I name the sequence between upstream 1988 bp and 2110 bp the epidermal enhancer. I tested the deletion of the epidermal enhancer from the longest upstream 4976 bp construct. This construct again showed *Kaede* expression in the epidermis, suggesting that another epidermal enhancer should be present between the upstream 2295 bp and 4976 bp (Fig. 8A).

4.7 Epidermal enhancer of *Ci-cdc25* is synergistically activated by the GATA, AP-2 and Sox binding sites

To identify potential regulatory sites in the epidermal enhancer, I compared the genomic sequences of the corresponding genomic region of the closely related species *Ciona savignyi*. I found that the two GATA binding sites, two AP-2 binding sites and three Sox binding sites are well conserved between the two species (Fig. 9A). I then examined whether these putative transcription factor binding sites are necessary for the activity of epidermal enhancer of *Ci-cdc25* by mutating or deleting these sites. When two GATA binding sites were mutated, expression of *Kaede* in the epidermis was suppressed, while mutation of one of these sites had weaker effect (Fig. 9B). These results suggest that the two GATA binding sites synergistically activate the epidermal enhancer. I noticed that the reporter expression was still observed even though two GATA binding sites were mutated. This result suggested that the binding sites other than GATA binding sites are also involved in the activation of epidermal enhancer. Therefore, I tested the effect of mutating or deleting the two AP-2 binding sites and three Sox binding sites in the sequence between upstream 1989 bp and 2110 bp. Mutating or deleting one of the two putative AP-2 binding sites resulted in a reduction of *Kaede* expression, while simultaneous deletions of the three Sox binding sites in addition to the deletion of the two AP-2 binding sites almost completely eliminate the epidermal expression of *Kaede* (Figs. 9B, C), suggesting their involvement in the activation of *Ci-cdc25* epidermal enhancer. Taken together, these results suggest that the epidermal enhancer of *Ci-cdc25* is activated synergistically through GATA, AP-2 and Sox transcription factors.

4.8 *Ci-AP2L2* directs epidermal differentiation at the downstream of GATA

In *Ciona*, the specification of ectoderm occurs from the 8-cell stage. Four animal cells (a4.2 and b4.2 pairs) are specified as ectoderm by the activity of two GATA transcription factors. There are two GATA orthologous genes in the *Ciona* genome. Both of them, *Ci-GATA-a* and *Ci-GATA-b* synergistically regulate the specification of epidermis (Rothbächer, et al., 2007). However, genes that regulate the differentiation of epidermis under the control of GATA transcription factors are not identified. The transcription factor AP-2 was initially identified as the transcription factor regulating the transcriptional activation of keratin genes, type of intermediate filament specific to vertebrate epidermis (Leask et al., 1990; Snape et al., 1991). The *Ciona* genome encodes genes closely related to keratin pairs, *Ci-IF-C* and *Ci-IF-D* both of which is strongly expressed in the tail epidermis (Karabinos et al., 2004). A repressor version of Ci-GATA-a, En-Ci-GATA-a can inhibit the expression of marker genes of epidermis (Rothbächer, et al., 2007). I found that the expression of *Ci-IF-C* and *Ci-IF-D* were also inhibited in the embryos injected with *En-Ci-GATA-a* mRNA (Fig. 10B). Among the two AP-2 homologues in the *Ciona* genome, *Ci-AP-2-like2* (*Ci-AP2L2*) shows conspicuous expression in the ectodermal precursor cells from the 16-cell stage (Imai et al., 2004; Fig. 17A), suggesting that this gene mediates the expression of *Ci-IF-C* and *Ci-IF-D* under the control of GATA transcription factors. To test the involvement of *Ci-AP2L2* in the activation of *Ci-IF-C* and *Ci-IF-D*, I knocked down *Ci-AP2L2* using morpholino oligonucleotides (MO). *Ci-AP2L2* MO disrupted the splicing of *Ci-AP2L2* and resulted in the generation of abnormal transcript (Fig. 14D). When I examined the expression of *Ci-IF-C* and *Ci-IF-D* by *in situ* hybridization in the embryos knocked down with *Ci-AP2L2*, the expression of *Ci-IF-C* and *Ci-IF-D* were reduced, and their

expression were rescued by co-injection of *Ci-AP2L2* mRNA (Fig. 10A). I also found that the repressor version of *Ci-AP2L2*, *En-Ci-AP2L2* efficiently inhibited the expression of *Ci-IF-C* and *Ci-IF-D* (Fig.10A). These results suggest that *Ci-AP2L2* regulates the differentiation of the epidermis in *Ciona*. Then I asked whether *Ci-AP2L2* induce the expression of *Ci-IF-C* and *Ci-IF-D*. As mentioned above, in the embryos blocked the activity of Ci-GATA-a, expression of *Ci-IF-C* and *Ci-IF-D* was disappeared (Fig. 10B). However, co-injection of *Ci-AP2L2* mRNA with *En-Ci-GATA-a* mRNA could recovered the expression of *Ci-IF-C* and *Ci-IF-D* (Fig. 10B), suggesting that *Ci-AP2L2* regulates the differentiation of the epidermis at the downstream of GATA transcription factors.

Next, I tested the function of *Ci-AP2L2* in the overall differentiation of epidermis. At first, I examined the expression of epidermis specific gene *Ci-Epi1* in embryos injected with *Ci-AP2L2* MO or *En-Ci-AP2L2*. However, the expression of *Ci-Epi1* was not reduced in these embryos (Fig. 10C). To further investigate the role of *Ci-AP2L2* in the differentiation of epidermis, I performed two experiments to assess whether *Ci-AP2L2* can induce the expression of *Ci-Epi1*. In the first experiment, I examined whether co-expressing *Ci-AP2L2* can reverse the inhibitory effect of *En-Ci-GATA-a* on the expression of *Ci-Epi1*. As a result, *Ci-Epi1* expression was recovered in embryos co-injected with *En-Ci-GATA-a* and *Ci-AP2L2* (Fig. 10C), suggesting that *Ci-AP2L2* is sufficient for inducing the expression of *Ci-Epi1* even when Ci-GATA-a is blocked. The previous study has shown that the activity of Ci-GATA-a is inhibited in the vegetal blastomeres by accumulating nuclear β-catenin from the 8-cell stage (Rothbächer, et al., 2007). 1-azakenpaullone is a potent ATP-competitive inhibitor of GSK-3β kinase (Kunick et al., 2004). Treatment of

embryos with this drug might vegetalize the embryo by constitutively activating the β-catenin signaling in vegetal blastomeres. Consistent with this idea, treating embryos with 1-azakenpaullone from the 8-cell stage could inhibit the expression of *Ci-Epi1* (Fig. 10D).

I then examined whether injection of *Ci-AP2L2* mRNA can recover the expression of *Ci-Epi1*. In the embryos injected with *Ci-AP2L2* mRNA the expression of *Ci-Epi1* was observed even the embryos were treated with 1-azakenpaullone from the 8-cell stage (Fig. 10D), suggesting that *Ci-AP2L2* is sufficient to induce the expression of *Ci-Epi1* in the vegetalized condition. Overall, these results suggest that *Ci-AP2L2* plays an important role in the overall differentiation of epidermis.

4.9 *Ci-AP2L2* and *Ci-GATA-b* synergistically activates the epidermal expression of *Ci-cdc25*

I next sought to identify the relationship between the cell fate determination and transcriptional activation of *Ci-cdc25* in epidermis. At first, I focused on *Ci-AP2L2*. Knockdown of *Ci-AP2L2* by the MO resulted in the reduction of *Ci-cdc25* expression in the epidermis at the gastrula stage (Figs. 11A) that could be reversed by co-injection of *Ci-AP2L2* mRNA (Fig. 18). However, the weak expression of *Ci-cdc25* in the epidermis was still observed in embryos knocked down with *Ci-AP2L2*, suggesting that another transcription factor regulates the epidermal expression of *Ci-cdc25*.

I then examined the knockdown of *Ci-GATA-b* because this gene shows strong zygotic expression at the gastrula stage (Fig. 17B). Knockdown of *Ci-GATA-b* by the MO resulted in the reduction of *Ci-cdc25* expression in the epidermis at the gastrula stage (Fig. 11A) that could be reversed by co-injection of *Ci-GATA-b* mRNA (Fig. 18).

Residual epidermal expression of *Ci-cdc25* in either the embryos in which *Ci-AP2L2* MO or *Ci-GATA-b* MO injected, suggests that *Ci-AP2L2* and *Ci-GATA-b* act synergistically on the epidermal expression of *Ci-cdc25*. Indeed, in the embryos co-injected with *Ci-AP2L2* MO and *Ci-GATA-b* MO, *Ci-cdc25* expression in the epidermis was further reduced (Fig. 11A), suggesting that *Ci-AP2L2* and *Ci-GATA-b* synergistically activate the expression of *Ci-cdc25* in the epidermis. In these embryos, *Ci-cdc25* expression in the notochord lineage was retained (Fig. 11B), demonstrating that *Ci-AP2L2* and *Ci-GATA-b* activates the transcription of *Ci-cdc25* in a cell type specific manner. I also knocked down one of the Sox transcription factors, *Ci-SoxB1* which shows epidermal expression at the gastrula stage (Imai et al., 2004) using MO (Fig. 15) and examined the effect on the epidermal expression of *Ci-cdc25*. However, injection of *Ci-SoxB1* MO results in slight reduction of *Ci-cdc25* expression in the epidermis (Fig. 18). I could not exclude the possibility that Sox transcription factors other than *Ci-SoxB1* is involved in the activation of *Ci-cdc25* transcription in the epidermis. The expression of *Ci-AP2L2*, *Ci-SoxB1* and *Ci-GATA-b* is observed as early as the 16-cell, 32-cell and 64-cell stage (Imai et al., 2004).

I then examined the expression of *Ci-cdc25* at the blastrula stage (24-cell, 32-cell and 64-cell) in the embryos knocked down with *Ci-AP2L2* and *Ci-SoxB1*. I found that knockdown of either of these genes did not affect the expression of *Ci-cdc25* in the precursor blastomeres of epidermis (Fig. 19). Overall, these results indicate that *Ci-AP2L2* and *Ci-GATA-b* regulate transcription of *Ci-cdc25* from the gastrula stage.

4.10 Knockdown of *Ci-AP2L2* and *Ci-GATA-b* caused the lengthening of epidermal cell cycle during gastrulation

The above results demonstrated that epidermal expression of *Ci-cdc25* is activated by the genetic program for epidermal differentiation. The expression of *Ci-AP2L2* and *Ci-GATA-b* was strong during gastrulation (Fig. 12A, 5hpf), while their expression was reduced during neurulation (Fig. 12A, 7hpf and 8hpf). To examine whether the expression of *Ci-AP2L2* and *Ci-GATA-b* is down-regulated, I quantified the expression of *Ci-AP2L2* and *Ci-GATA-b* to find that these transcription factors are indeed down-regulated during neurulation (Fig. 12B). The timing when *Ci-AP2L2* and *Ci-GATA-b* are down-regulated corresponds with the timing when *Ci-cdc25* is down-regulated (Figs. 3A, B and 12A, B). Therefore, I examined whether the down-regulation of *Ci-AP2L2* and *Ci-GATA-b* can facilitates the interphase lengthening of epidermal cells. I injected C*i-AP2L2* MO and *Ci-GATA-b* MO and examined the effect on the interphase length of epidermal cells. The effect of *Ci-GATA-b* MO injection was not apparent (Fig. 12C) while *Ci-AP2L2* MO injection resulted in increase of the 10th interphase length up to 14.8 min (23.2%) (Fig. 12D). Co-injecting MOs against *Ci-AP2L2* and *Ci-GATA-b* resulted in further increase of the 10th interphase length up to 23.8 min (38.8%) (Fig. 12E). Injection of *Ci-AP2L2* MO and *Ci-GATA-b* MO did not significantly affect the M-phase length (Fig. 20). These results suggest that down-regulation of *Ci-AP2L2* and *Ci-GATA-b* which occurs when embryos progress from the gastrula stage to the neurula stage, facilitates the interphase lengthening of epidermal cells. If the down-regulation of *Ci-AP2L2* and *Ci-GATA-b* facilitates the interphase lengthening of epidermal cells by causing the down-regulation of *Ci-cdc25*, overexpressing *Ci-AP2L2* mRNA or *Ci-GATA-b* mRNA could postpone *Ci-cdc25*

down-regulation which occurs at the onset of neurulation in normal embryos. Indeed, overexpression of *Ci-AP2L2* mRNA caused apparent increase in the epidermal expression of *Ci-cdc25* at the neurula stage (Fig. 12F), suggesting that the down-regulation of *Ci-AP2L2* is a required for *Ci-cdc25* down-regulation at the onset of neurulation. On the other hand, overexpression of *Ci-GATA-b* did not increase the expression of *Ci-cdc25* at the neurula stage (Fig. 12F). Taken together, these results suggest that *Ci-AP2L2* and *Ci-GATA-b* synergistically regulates the interphase length of epidermal cells. It is also suggested that down-regulation of *Ci-AP2L2* is required for *Ci-cdc25* down-regulation at the onset of neurulation.

5. Discussion

5.1 Role of interphase lengthening of epidermal cells in neurulation

It is thought that the timing of mitosis during morphogenesis must be carefully regulated, because morphogenetic movement of a cell can be interrupted when the cell enters mitosis (Duncan and Su, 2004). When a cell enters mitosis, cytoskeletal reorganization which is incompatible with cell shape changes require for morphogenetic cell movement occurs. For example, a kind of cell shape change, apical constriction, which is driven by apically accumulated F-actin contractile ring (Sawyer et al., 2010), observed during gastrulation in *Drosophila* can be interfered with precocious mitoses (Großhans and Wieschaus, 2000). To avoid the interference, cell cycle must be arrested in mesodermal cells during gastrulation for proper morphogenesis to occur.

In this study, I characterized the cell movement and mitosis of epidermal cells during the morphogenetic movement of neurulation. I discovered that when the left and right neural folds meet at the dorsal midline, the epidermal cells at the dorsal midline

perform characteristic changes of cell shape with concomitant F-actin accumulation at the leading edge. This F-actin accumulation is an active process, because the activity of Rho/ROCK signaling is required for the F-actin accumulation. Overexpression of *Ci-cdc25* shortened the interphase length of the epidermal cells. When precocious mitoses were induced by means of *Ci-cdc25* overexpression during the fusion of neural folds, the dorsal midline epidermal cells failed to accumulates F-actin at the leading edge and the elongation and movement of the dorsal midline epidermal cells were disrupted. Treating these *Ci-cdc25* overexpressed embryos with aphidicolin postponed mitoses of epidermal cells until after neurulation. In these embryos, accumulation of F-actin at the leading edge of the dorsal midline epidermal cells and concomitant elongation and cell movement were recovered. Thus I demonstrated that sufficient interphase length of epidermal cells is necessary to allow F-actin mediated movement of the dorsal midline epidermal cells for proper neurulation (Fig. 13A).

5.2 Transcriptional regulation of *Ci-cdc25* in the regulation of interphase length of epidermal cells

The present data suggests that *Ci-cdc25* promotes interphase progression in the epidermal cells through accelerating S-phase progression and shortening G2 phase. As in other eukaryotic cells, *cdc25* orthologue in *Ciona*, *Ci-cdc25* might regulate the interphase length of epidermal cells by modulating the activity of Cdk1. In *Drosophila*, interphase length during the blastoderm is regulated by the balance between phospho-inhibition of Cdk1 activity by Wee1 kinase and its release by Cdc25 phosophatase (Stumpff et al., 2004; Farrell et al., 2012). The interphase lengthening is thought to be a consequence of reduced Cdk1 activity. At the mid-blastrula transition

(MBT) in *Drosophila*, two isoforms of *cdc25* mRNA and Cdc25 protein are degraded (Edgar and Datar, 1996; Farrell and O'Farrell, 2013). It was recently shown that degradation of Cdc25/Twine protein is critical for the interphase lengthening (Farrell and O'Farrell, 2013). In *Xenopus*, *cdc25* mRNA and Cdc25 protein are degraded at the MBT, although which is responsible for the interphase lengthening at the MBT is still unknown (Kim et al., 1999).

In this study, I showed that *Ci-cdc25* mRNA is down-regulated as embryos progress from the gastrula stage to the neurula stage. The down-regulation of *Ci-cdc25* mRNA is at least in part responsible for the interphase lengthening of the epidermal cells. In *Drosophila*, regulation of *cdc25/string* transcription play important role in the regulation of interphase length especially after the gastrulation (Lehman et al., 1999). Indeed, recent study based on quantitative fluorescent imaging and computational modeling suggests that *cdc25/string* transcription triggers the decision of mitotic entry during gastrulation (Di Talia and Wieschaus, 2012). This mechanism is different from the one proposed from the experiments in *Xenopus* egg extract that the abrupt activation of Cdk1 at the onset of mitosis is regulated by two feedback loops: a positive feedback loop between Cdc25 and Cdk1 and a double negative feedback loop between Wee1 and Cdk1 (Sha et al., 2003). There seems to be several mechanisms to translate Cdc25 activity into interphase length during embryogenesis. The present study showed that *Ci-cdc25* transcription regulated by the transcription factors *Ci-AP2L2* and *Ci-GATA-b* plays a role in the control of interphase length of the epidermal cells (Fig.13B). To reveal whether *Ci-cdc25* transcription regulated by these transcription factors limits the timing of mitosis in epidermal cell, further investigation will be needed. Moreover, *Ci-cdc25* down-regulation was delayed in embryos elevated the amount of *Ci-AP2L2*

mRNA. Therefore, down-regulation of *Ci-AP2L2* at the onset of neurulation might be critical for the *Ci-cdc25* down-regulation during neurulation (Fig. 13C).

5.3 The genetic program for cell fate determination of epidermis in *Ciona*

In *Ciona*, epidermis is initially specified by the activity of maternal *Ci-GATA-a*. The activity of *Ci-GATA-a* is thought to be supplemented by the activity of zygotically expressed *Ci-GATA-b*. Even though maternal *Ci-GATA-a* mRNA is ubiquitously distributed in the egg, ectoderm formation is restricted in the animal blastomeres through the inhibition of Ci-GATA-a in the vegetal blastomeres by accumulating nuclear β-catenin (Rothbächer et al., 2007). GATA activity is thought to be permissive rather than instructive, because interference with Ci-GATA-a function has no effect on the early vegetal program and ectopic Ci-GATA-a expression does not impose the ectodermal program on vegetal cells (Rothbächer et al., 2007). Since a permissive activator cannot induce tissue differentiation by itself, another cell type specific transcription factor is necessary for the differentiation of epidermis. *Ci-AP2L2* is specifically expressed in the epidermal cells and a part of neural fated cells. Through knockdown and induction experiments, we showed that *Ci-AP2L2* is necessary and sufficient for the induction of epidermal marker genes. Thus, *Ci-AP2L2* might act in concert with (most likely at the downstream of) Ci-GATA-a in the differentiation of the epidermis (Fig.13B). Keratin genes are well studied structural component of epidermis in vertebrates (Leask et al., 1990; Snape et al., 1991). I noticed that the expression of keratin orthologous genes was excluded from the trunk epidermis, even though *Ci-AP2L2* is expressed in the anterior and posterior animal blastomeres that are fated to trunk and tail epidermis, respectively (Fig.17A). It is known that, by the 8-cell stage, the

anterior and posterior animal blastomeres have acquired different properties, including a differential responsiveness to inducing signals from the underlying mesendoderm, which depends on Ci-FoxA activity in the anterior animal blastomeres (Lamy et al., 2006). Exclusion of the expression of keratin orthologous genes from trunk epidermis might be achieved through the genetic program downstream of Ci-FoxA.

5.4 Coordination of cell cycle and cell fate determination of epidermal cells during neurulation

Cell type specific transcription factors play critical role in tissue formation during the embryogenesis of *Ciona* (Nishida, 2005). However, their role in the regulation of cell cycle during morphogenetic processes such as neurulation is largely unknown. Ci-AP2L2 and Ci-GATA-b are cell type specific transcription factors whose mRNA is expressed in the epidermal cells. The present study demonstrated that AP-2 and GATA act through the *cis*-regulatory element located upstream of *Ci-cdc25* in the coordination of cell cycle and cell fate determination of epidermal cells. The activities of Ci-AP2L2 and Ci-GATA-b should be tightly regulated during neurulation, because these transcription factors can activate *cdc25* transcription thereby shortening interphase length of epidermal cells.

I found that increasing the amount of *Ci-AP2L2* mRNA by microinjection interfere the down-regulation of *Ci-cdc25* in the epidermis at the onset of neurulation. In contrast, microinjecting *Ci-GATA-b* mRNA could not up-regulate *Ci-cdc25*. This difference may reflect permissive nature of *Ci-GATA-b* and instructive nature of *Ci-AP2L2* on the transcription of *Ci-cdc25*, as discussed for the cell fate determination of epidermis in the previous section. Alternatively, the activity of Ci-GATA-b may be

post-transcriptionally inhibited during neurulation. Interestingly, transcription factors AP-2 and GATA have been implicated in numerous human cancers (Hilger-Eversheim et al, 2000; Zheng et al., 2011). Their oncogenic potentials lie in their multiple functions to promote cell proliferation and cell differentiation. Therefore, deregulations of their activities are related to oncogenesis. The activities of AP-2 and GATA should also be tightly regulated during neurulation in *Ciona*, because these transcription factors affect the interphase length of epidermal cells through transcriptional regulation of *Ci-cdc25*. The *cis*-regulatory element of *Ci-cdc25* might activate *Ci-cdc25* transcription according to the concentration of AP-2 and GATA. Thus, cell cycle and cell fate determination of epidermal cells is coordinated by coupling these cell behaviors by the *cis*-regulation of *Ci-cdc25* during neurulation in *Ciona*.

6 Acknowledgments

I would like to acknowledge Dr. Asako Sakaue-Sawano and Dr. Atsushi Miyawaki at the RIKEN Brain Science Institute, Masashi Nakagawa at the University of Hyogo, the members of the Shimoda Marine Research Center at the University of Tsukuba for their kind cooperation with this study. I also thank National Bio-resource Project, MEXT, S. Fujiwara, and all members of the Maizuru Fishery Research Station of Kyoto University, the Education and Research Center of Marine Bioresources of Tohoku University and Misaki Marine Biological Station of the University of Tokyo for providing me with *Ciona* adults. This study was supported by Grants-in-Aid for Scientific Research from JSPS to Y.O. and Y.S. (No. 11J00127 and No.23681039). This study was further supported by grants from the National Bioresource Project.

7 References

Akanuma, T., Hori, S., Darras, S. and Nishida, H. (2002). Notch signaling is involved in neurogenesis in the ascidian embryos. *Dev. Genes Evol.* **212**, 459-472.

Bertrand, V., Hudson, C., Caillol, D., Popovici, C. and Lemaire, P. (2003). Neural tissue in ascidian embryos is induced by FGF9/16/20, acting via a combination of maternal GATA and Ets transcription factors. *Cell* **115**, 615-627.

Budirahardja, Y. and Gönczy, P. (2009). Coupling the cell cycle to development. *Development* **136**, 2861-2872.

Chen, Z. F. and Behringer, R. R. (1995). Twist is required in head mesenchyme for cranial neural tube morphogenesis. *Genes Dev.* **9**, 686-699.

Chiba, S., Satou, Y., Nishikata, T. and Satoh, N. (1998). Isolation and characterization of cDNA clones for genes in *Ciona savignyi* embryos. *Zool. Sci.* **246**, 239-246.

Cole, A. G. and Meinertzhagen, I. A. (2004). The central nervous system of the ascidian larva: mitotic history of cells forming the neural tube in late embryonic Ciona intestinalis. *Dev. Biol.* **271**, 239-262.

Copp, A.J., Brook, F. A. and Roberts, H. J. (1988). A cell-type-specific abnormality of cell proliferation in mutant (curly tail) mouse embryos developing spinal neural tube defects. *Development* **104**, 285-295.

Copp, A. J., Greene, N. D. E. and Murdoch, J. N. (2003). The genetic basis of mammalian neurulation. *Nature Rev. Genetics* **4**, 784-793.

Corbo, J. C., Erives, A., Di Gregorio, A., Chang, A. and Levine, M. (1997). Dorsoventral patterning of the vertebrate neural tube is conserved in a protochordate. *Development* **124**, 2335-2344.

Di Talia, S., She, R., Blythe, S. a, Lu, X., Zhang, Q. F. and Wieschaus, E. F. (2012). Posttranslational control of Cdc25 degradation terminates *Drosophila*'s early cell-cycle program. *Curr. Biol.* **27**, 127-132.

Duncan, T. and Su, T. T. (2004). Embryogenesis: coordinating cell division with gastrulation. *Curr. Biol.* **14**, R305-R307.

Edgar, B. A. and Datar, S. A. (1996). Zygotic degradation of two maternal Cdc25 mRNAs terminates *Drosophila*'s early cell cycle program. *Genes Dev.* **10**, 1966-1977.

Edgar, B. A. and O'Farrell, P. H. (1990). The three postblastoderm cell cycles of *Drosophila* embryogenesis are regulated in G2 by string. *Cell* **62**, 469-480.

Farrell, J. A, Shermoen, A. W., Yuan, K. and O'Farrell, P. H. (2012). Embryonic onset of late replication requires Cdc25 down-regulation. *Genes Dev.* **26**, 714-725.

Farrell, J. A, and O'Farrell, P. H. (2013). Mechanism and regulation of Cdc25/Twine protein destruction in embryonic cell-cycle remodeling. *Curr. Biol.* **23**, 118-126.

Foe, V. E. and Odell, G. M. (1989). Mitotic domains partition in fly embryos, reflecting early cell biological consequences of determination in progress. *Amer. Zool.* **29**, 617-652.

Frazer, K. A, Pachter, L., Poliakov, A., Rubin, E. M. and Dubchak, I. (2004). VISTA: computational tools for comparative genomics. *Nucleic Acids Res.* **32**, 273-279.

Fukano, T., Sawano, A., Ohba, Y., Matsuda, M. and Miyawaki, A. (2007). Differential Ras activation between caveolae/raft and non-raft microdomains. *Cell Struct. Funct.* **32**, 9-15.

Großhans, J., and Wieschaus, E. (2000). A Genetic link between morphogenesis and cell division during formation of the ventral furrow in *Drosophila*. *Cell* **101**, 523-531.

Gustavsson, P., Greene, N. D. E., Lad, D., Pauws, E., de Castro, S. C. P., Stanier, P., and Copp, A. J. (2007). Increased expression of *Grainyhead-like-3* rescues spina bifida in a folate-resistant mouse model. *Human Mol. Gen.* **16**, 2640-2646.

Hilger-Eversheim, K., Moser, M., Schorle, H. and Buettner, R. (2000). Regulatory roles of AP-2 transcription factors in vertebrate development, apoptosis and cell-cycle control. *Gene* **260**, 1-12.

Hotta, K., Mitsuhara, K., Takahashi, H., Inaba, K., Oka, K., Gojobori, T. and Ikeo, K. (2007). A web-based interactive developmental table for the ascidian *Ciona*

intestinalis, including 3D real-image embryo reconstructions: I. From fertilized egg to hatching larva. *Dev. Dyn.* **236**, 1790-1805.

Hozumi, A., Kawai, N., Yoshida, R., Ogura, Y., Ohta, N., Satake, H., Satoh, N. and Sasakura, Y. (2010). Efficient transposition of a single Minos transposon copy in the genome of the ascidian *Ciona intestinalis* with a transgenic line expressing transposase in eggs. *Dev. Dyn.* **239**, 1076-1088.

Hozumi, A., Yoshida, R., Horie, T., Sakuma, T., Yamamoto, T. and Sasakura, Y. (2013). Enhancer activity sensitive to the orientation of the gene it regulates in the chordate genome. *Dev. Biol.* **375**, 79-91.

Hudson, C., and Lemaire, P. (2001). Induction of anterior neural fates in the ascidian *Ciona intestinalis*. *Mech. Dev.* **100**, 189-203.

Ikegami, S., Taguchi, T., Ohashi, M., Oguro, M., Nagano, H. and Mano, Y. (1978). Aphidicolin prevents mitotic cell division by interfering with the activity of DNA polymerase-alpha. *Nature* **275**, 458-460.

Imai, K. S., Hino, K., Yagi, K., Satoh, N. and Satou, Y. (2004). Gene expression profiles of transcription factors and signaling molecules in the ascidian embryo: towards a comprehensive understanding of gene networks. *Development* **131**, 4047-4058.

Imai, K. S., Levine, M., Satoh, N. and Satou, Y. (2006). Regulatory blueprint for a chordate embryo. *Science* **312**, 1183-1187.

Karabinos, A., Zimek, A. and Weber, K. (2004). The genome of the early chordate *Ciona intestinalis* encodes only five cytoplasmic intermediate filament proteins

including a single type I and type II keratin and a unique IF - annexin fusion protein. *Gene* **326**, 123-129.

Kawashima, T., Tokuoka, M., Awazu, S., Satoh, N., and Satou, Y. (2003). A genomewide survey of developmentally relevant genes in *Ciona intestinalis*. VIII. Genes for PI3K signaling and cell cycle. *Dev. Genes. Evol.* **213**, 284-290.

Kim, S. H., Li, C. and Maller, J. L. (1999). A maternal form of the phosphatase Cdc25A regulates early embryonic cell cycles in *Xenopus laevis*. *Dev. Biol.* **212**, 381-391.

Kunick, C., Lauenroth, K., Leost, M., Meijer, L. and Lemcke, T. (2004). 1-Azakenpaullone is a selective inhibitor of glycogen synthase kinase-3β. *Bioorg. Med. Chem. Lett.* **14**, 413-416.

Lamy, C., Rothbächer, U., Caillol, D. and Lemaire, P. (2006). *Ci-FoxA-a* is the earliest zygotic determinant of the ascidian anterior ectoderm and directly activates *Ci-sFRP1/5*. *Development* **2844**, 2835-2844.

Leask, A, Rosenberg, M., Vassar, R. and Fuchs, E. (1990). Regulation of a human epidermal keratin gene: sequences and nuclear factors involved in keratinocyte-specific transcription. *Genes Dev.* **4**, 1985-1998.

Lehman, D. A, Patterson, B., Johnston, L. A, Balzer, T., Britton, J. S., Saint, R. and Edgar, B. A. (1999). *Cis*-regulatory elements of the mitotic regulator, *string/Cdc25*. *Development* **126**, 1793-1803.

Lemaire, P., Garrett, N. and Gurdon, J.B. (1995). Expression cloning of *Siamois*, a *Xenopus* homeobox gene expressed in dorsal-vegetal cells of blastulae and able to induce a complete secondary axis. *Cell* **81**, 85-94.

Leonhardt, H., Rahn, H. P., Weinzierl, P., Sporbert, A, Cremer, T., Zink, D. and Cardoso, M. C. (2000). Dynamics of DNA replication factories in living cells. *J. Cell Biol.* **149**, 271-280.

Leung, L., Klopper, A. V., Grill, S. W., Harris, W. A. and Norden, C. (2011). Apical migration of nuclei during G2 is a prerequisite for all nuclear motion in zebrafish neuroepithelia. *Development* **138**, 5003-5013.

Lowery, L. A. and Sive, H. (2004). Strategies of vertebrate neurulation and a reevaluation of teleost neural tube formation. *Mech. Dev.* **121**, 1189-1197.

Malumbres, M. and Barbacid, M. (2009). Cell cycle, CDKs and cancer: a changing paradigm. *Nat. Rev. Cancer*, **9**, 153-166.

McCleland, M. L., Shermoen, A. W. and O'Farrell, P. H. (2009). DNA replication times the cell cycle and contributes to the mid-blastula transition in Drosophila embryos. *J. Cell Biol.* **187**, 7-14.

Nagai, T., Ibata, K, Park, E.S., Kubota, M., Mikoshiba, K. and Miyawaki, A. (2002). A variant of yellow fluorescent protein with fast and efficient maturation for cell-biological applications. *Nat. Biotechnol.* **20**, 87-90.

Nicol, D. and Meinertzhagen, I. A. (1988) Development of the central nervous system of the larva of the ascidian, *Ciona intestinalis* L. II. Neural plate morphogenesis and cell lineages during neurulation. *Dev. Biol.* **130**, 737-766.

Nishida, H. (2005). Specification of embryonic axis and mosaic development in ascidians. *Dev. Dyn.*, **233(4)**, 1177-1193.

Nottoli, T., Hagopian-Donaldson, S., Zhang, J., Perkins, A, and Williams, T. (1998). AP-2-null cells disrupt morphogenesis of the eye, face, and limbs in chimeric mice. *Proc. Natl. Acad. Sci. U.S.A.* **95**, 13714-13719.

Nogare, D. E. D., Arguello, A., Sazer, S. and Lane, M. E. (2007). Zebrafish *cdc25a* is expressed during early development and limiting for post-blastoderm cell cycle progression. *Dev. Dyn.* **236**, 3427-3435.

Philipova, R., Kisielewska, J., Lu, P., Larman, M., Huang, J.-Y. and Whitaker, M. (2005). ERK1 activation is required for S-phase onset and cell cycle progression after fertilization in sea urchin embryos. *Development* **132**, 579-589.

Raftopoulou, M., and Hall, A. (2004). Cell migration: Rho GTPases lead the way. *Dev. Biol.* **265**, 23-32.

Rothbächer, U., Bertrand, V., Lamy, C. and Lemaire, P. (2007). A combinatorial code of maternal GATA , Ets and β-catenin- TCF transcription factors specifies and patterns the early ascidian ectoderm. *Development* **4032**, 4023-4032.

Roure, A., Rothbächer, U., Robin, F., Kalmar, E., Ferone, G., Lamy, C., Missero, C., Mueller, F. and Lemaire, P. (2007). A multicassette Gateway vector set for high throughput and comparative analyses in *Ciona* and vertebrate embryos. *PloS One* **2**, e916.

Sakaue-Sawano, A., Kurokawa, H., Morimura, T., Hanyu, A., Hama, H., Osawa, H., Kashiwagi, S., Fukami, K., Miyata, T., Miyoshi, H., Imamura, T., Ogawa, M., Masai, H. and Miyawaki, A. (2008). Visualizing spatiotemporal dynamics of multicellular cell-cycle progression. Cell **132**, 487-498.

Sasakura, Y., Awazu, S., Chiba, S. and Satoh, N. (2003). Germ-line transgenesis of the Tc1/mariner superfamily transposon *Minos* in *Ciona intestinalis*. *Proc. Natl. Acad. Sci. U.S.A.* **100,** 7726-7730.

Sawyer, J. M., Harrell, J. R., Shemer, G., Sullivan-Brown, J., Roh-Johnson, M. and Goldstein, B. (2010). Apical constriction: a cell shape change that can drive morphogenesis. *Dev. Biol.* **341**, 5-19.

Schorle, H., Meier, P., Buchert, M., Jaenische, R. and Mitchell, P.J. (1996). Transcription factor AP-2 essential for cranial closure and craniofacial development. *Nature* **381**, 235-238.

Sha, W., Moore, J., Chen, K., Lassaletta, A. D., Yi, C.-S., Tyson, J. J. and Sible, J. C. (2003). Hysteresis drives cell-cycle transitions in *Xenopus laevis* egg extracts. *Proc. Natl. Acad. Sci. USA*, **100(3)**, 975-980.

Smith, J. L. and Schoenwolf, G. C. (1988) Role of cell-cycle in regulating neuroepithelial cell shape during bending of the chick neural plate. *Cell Tissue Res.* **252**, 491-500.

Snape, A. M., Winning, R. S. and Sargent, T. D. (1991). Transcription factor AP-2 is tissue-specific in *Xenopus* and is closely related or identical to keratin transcription factor 1 (KTF-1). *Development* **113**, 283-293.

Stumpff, J., Duncan, T., Homola, E., Campbell, S. D. and Su, T. T. (2004). *Drosophila* Wee1 kinase regulates Cdk1 and mitotic entry during embryogenesis, *Curr.Biol.* **14**, 2143-2148.

Tarallo, R. and Sordino, P. (2004). Time course of the programmed cell death in *Ciona intestinalis* in relation to mitotic activity and MAPK signaling. *Dev. Dyn.* **230**, 251-262.

Uehata, M., Ishizaki, T., Satoh, H., Ono, T., Kawahara, T., Morishita, T., Tamakawa, H., Yamagami, K., Inui, J., Maekawa, M. and Narumiya, S. (1997). Calcium sensitization of smooth muscle mediated by a Rho-associated protein kinase in hypertension. *Nature* **389**, 990-994.

Ueno, H., Nakajo, N., Watanabe, M., Isoda, M. and Sagata, N. (2008). FoxM1-driven cell division is required for neuronal differentiation in early *Xenopus* embryos. *Development* **135**, 2023-2030.

Wickramasinghe, D., Becker, S., Ernst, M. K., Resnick, J. L., Centanni, J. M., Tessarollo, L., Grabel, L. B. and Donovan, P. J.(1995). Two CDC25

homologues are differentially expressed during mouse development. *Development* **121**, 2047-2056.

Yamada, A. and Nishida, H. (1999). Distinct parameters are involved in controlling the number of rounds of cell division in each tissue during ascidian embryogenesis. *J. Exp Zool.* **84**, 379-391.

Yasuo, H. and Satoh, N. (1993). Function of vertebrate T gene. *Nature* **364**, 582-583.

Zheng, R. and Blobel, G. A. (2010). GATA transcription factors and cancer. *Genes Cancer* **1**, 1178-1188.

8 Tables

Table 1. Intervals between the 9th, 10th and 11th mitosis of epidermal cells

Mitotic domain	Interval between 9th and 10th mitosis* (min)					Interval between 10th and 11th mitosis* (min)								
	50	55	60	65	mean	80	85	90	95	100	105	110	115	mean
MD1	0	4	8	4	60	0	1	3	7	2	2	1	0	96.3
MD2	4	6	2	2	55.7	1	0	5	2	3	0	3	0	96.4
MD3b	4	6	2	2	55.7	0	2	1	2	4	3	1	1	99.3
MD3a	0	2	20	4	60.4	0	0	0	0	0	13	12	1	107.7

*Number of cells with the corresponding interval length is shown.

Table 2. *Ci-cdc25* overexpression disrupts neural tube closure

Experiment number	Trunk+tail*	Trunk**	Completed***	Total
1	4	2	3	9
2	2	4	1	7
3	4	4	1	9
Total	10 (40%)	10 (40%)	5 (20%)	25

*Number of embryos with defects in neural tube closure at both trunk and tail.

**Number of embryos with defects in neural tube closure at trunk.

***Number of embryos with completed neural tube closure.

Table 3. Aphidicolin treatment prevents defects in neurulation in the tail region.

Experiment number	Treatment	Normal***	Defects****
1	*Ci-cdc25* OE+DMSO*	3	5
	Ci-cdc25 OE +aphidicolin**	8	0
2	*Ci-cdc25* OE +DMSO	0	6
	Ci-cdc25 OE +aphidicolin	5	3

**Ci-cdc25*-overexpressing embryos treated with DMSO from 7.0 hpf.

***Ci-cdc25*-overexpressing embryos treated with aphidicolin from 7.0 hpf.

***Number of embryos with normal neural tube closure in the tail region.

****Number of embryos with defects in neural tube closure in the tail region.

Aph, aphidicolin; DMSO, dimethyl sulfoxide; OE, overexpression.

9 Figures

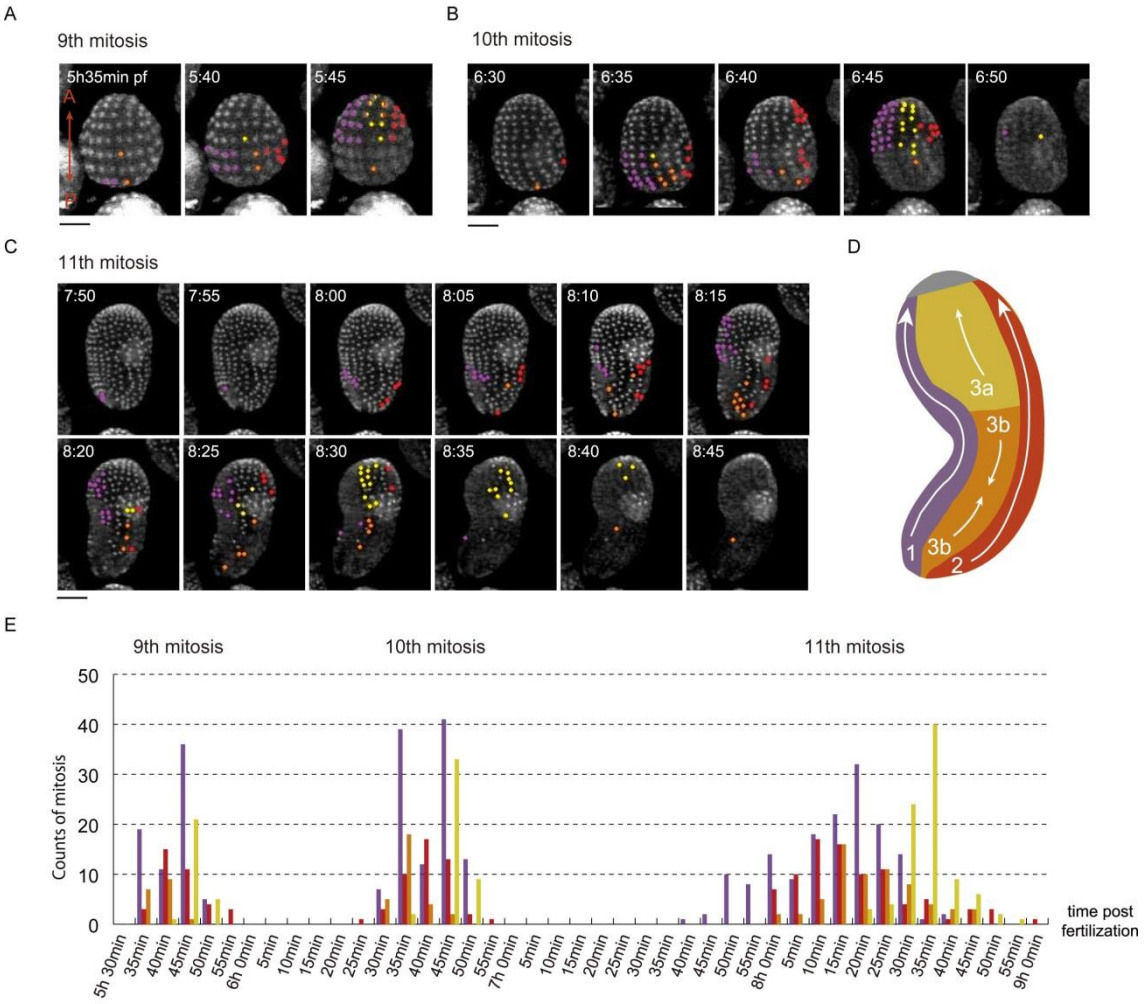

Figure 1

Fig. 1. Mitotic timing of epidermal cells during neurulation. mAG-hGem(1/110) mRNA-introduced embryos were subjected to time-lapse imaging at 5-min intervals. Nuclei of the cells entered into the prometaphase in the next 5-min interval were marked with dots. The colors of the dots correspond to the mitotic domains shown in (D). An embryo at the center was viewed from the lateral side. (A) Timing of the 9th mitosis. The A-P axis of the embryo is indicated by a double-headed arrow. Black bar, 50 μm. (B) Timing of the 10th mitosis. (C) Timing of the 11th mitosis. (D) A schematic diagram of mitotic domains of the epidermal cells of tailbud-stage embryos. The four mitotic domains, MD1, MD2, MD3a and MD3b, are observed. The patterns of progression of mitosis in each mitotic domain are shown by arrows. (E) Histogram representing the timing for epidermal cells to enter the prometaphase of the 9th, 10th, and 11th mitosis. The colors of the bars correspond to the mitotic domains in (D).

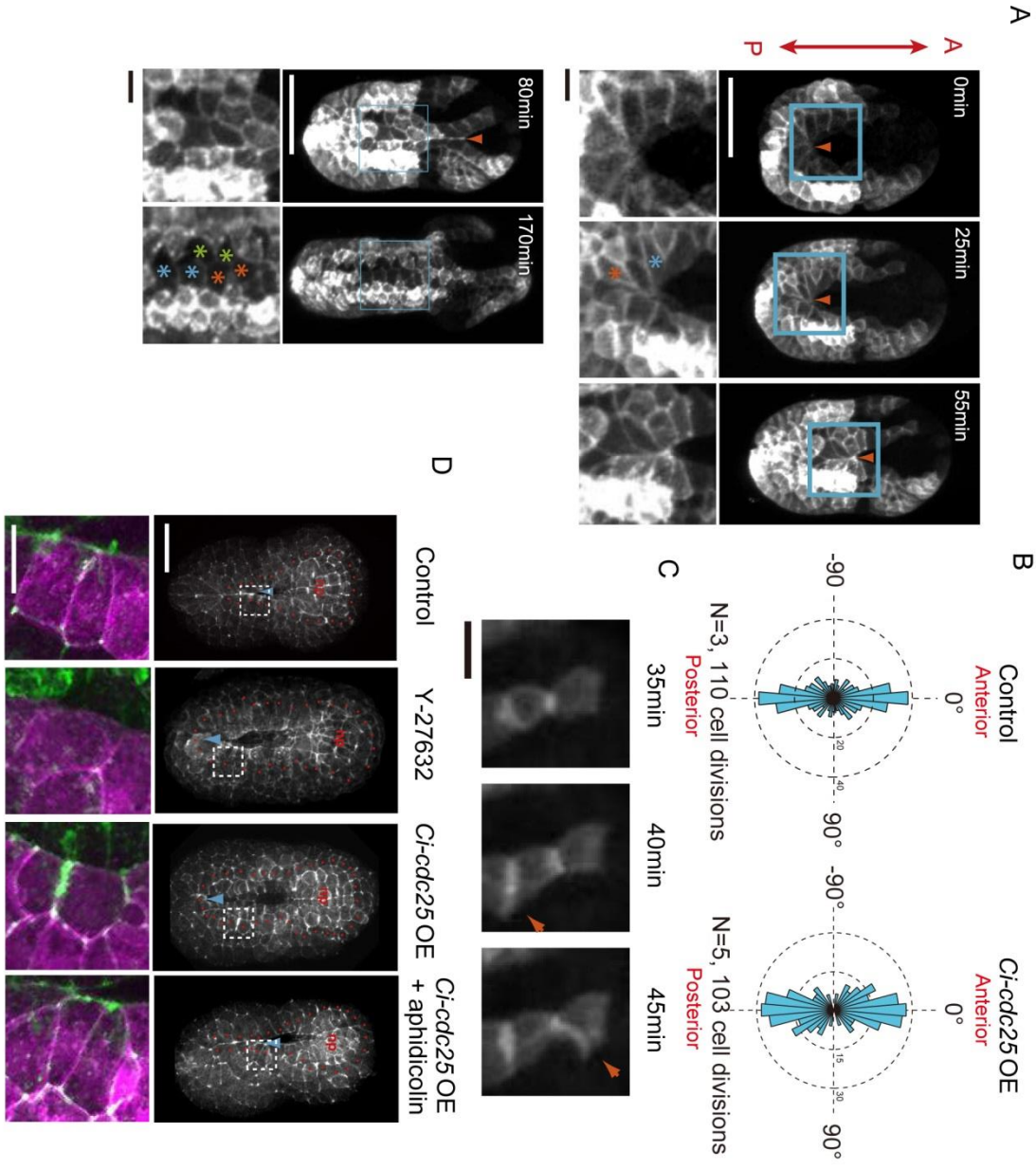
A
A
P
0min
25min
55min
80min
170min
B
Control
Anterior
0°
-90°
90°
N=3, 110 cell divisions
Posterior
Ci-cdc25 OE
Anterior
0°
-90°
90°
N=5, 103 cell divisions
Posterior
C
35min
40min
45min
D
Control
Y-27632
Ci-cdc25 OE
Ci-cdc25 OE
+ aphidicolin

Figure 2

Fig. 2. Fusion of epidermis during neurulation occurs at the interphase of the eleventh cell cycle. (A) Cell shape changes of epidermal cells during neural tube closure, as revealed by fluorescence of Kaede-CAAX fusion driven by the *Ci-Epi1* promoter. The upper column shows the entire embryo, while the lower column shows the magnified view of the area indicated by the squares in the upper column. At 25 min, the posterior cells of the dorsal epidermis elongated toward the anterior (red asterisk) and the cells at the lateral side elongated laterally (blue asterisk). These cells made contact at the focus (arrowhead). At 55 min, the neural tube of the tail was closed. The cellular focus at the zippering origin moved toward the anterior (arrowhead). At 80 min, half of the trunk midline was closed. The 11th mitosis of the midline epidermal cells occurred in parallel to the A-P axis (t = 170). The 11th mitosis of three cells was tracked, and their daughter cells are marked with the same colored asterisks. Bar, 50 μm for the upper column and 10 μm for the lower column. (B) Epidermal cells tend to divide parallel to the A-P axis at the 11th mitosis. (left) An example of measurement of the angle between the mitosis orientation and the A-P axis. A pair of sister cells just after the 11th mitosis (the square in the upper column) is shown at bottom. The angle (θ) is 15^{o} in this case (right). Rose diagrams of the orientation of 11th mitosis of the control embryos and *Ci-cdc25* overexpressed embryos. Division angles with respect to the A-P axis are binned from - 180^{o} to + 180^{o} in bins of 10^{o}. (C) Filopodia formation of the dorsal midline epidermal cells during neural tube closure. At 40 - 45 minutes after imaging was started, filopodia (arrowheads) were elongated towards the midline. Scale bar: 10 μm. (D) Accumulation of F-actin at the medial end of the dorsal midline epidermis is disrupted by Y-27632 treatment and overexpression of *Ci-cdc25*. In the upper row, fluorescent image of an F-actin stained embryo detected with

Alexa-488-phalloidin is shown in grayscale. The embryo was fixed at 8.0 hpf. Magnified images of the area shown with dotted squares are shown in color (insets) in order to show the boundary between the dorsal midline epidermis and the neural plate. Staining with Alexa-488-phalloidin is shown in green. Plasma membrane of epidermal cells was labeled with mCherry-CAAX fusion proteins is shown in magenta, which were driven by a promoter of *Ci-Epi1*. The position of the dorsal midline epidermal cells is shown with red spots. In control embryos, strong accumulation of F-actin was observed at the medial end, which was abolished by Y-27632 treatment and overexpression of *Ci-cdc25*.F-actin accumulation was restored in *Ci-cdc25*-overexpressed and aphidicolin-treated embryos.

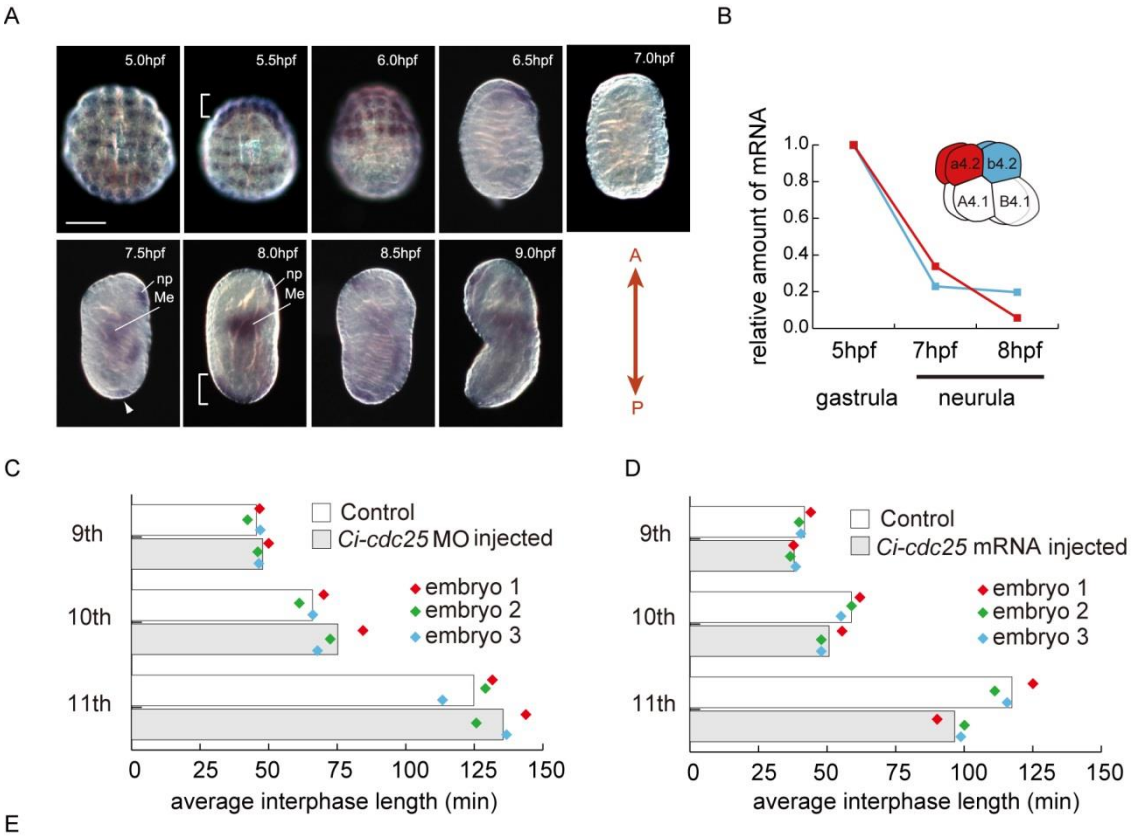
A
5.0hpf
5.5hpf
6.0hpf
6.5hpf
7.0hpf
7.5hpf
np
Me
8.0hpf
np
Me
8.5hpf
9.0hpf
A
P
B
relative amount of mRNA
1.0
0.8
0.6
0.4
0.2
0.0
a4.2
b4.2
A4.1
B4.1
5hpf
7hpf
8hpf
gastrula
neurula
C
9th
10th
11th
Control
Ci-cdc25 MO injected
embryo 1
embryo 2
embryo 3
0
25
50
75
100
125
150
average interphase length (min)
D
9th
10th
11th
Control
Ci-cdc25 mRNA injected
embryo 1
embryo 2
embryo 3
0
25
50
75
100
125
150
average interphase length (min)
E
Control
Ci-cdc25 mRNA injected
0:00
0:08
0:10
0:14
0:18
0:24
0:32
0:48
1:10

Figure 3

Fig. 3. *Ci-cdc25* regulates the interphase length of epidermal cells.

(A) Embryos fixed at 30 minute intervals between 5.0 and 9.0 hpf were examined by whole-mount *in situ* hybridization. Embryos are viewed from the animal side (5.0hpf - 6.0hpf) or lateral side (6.5 hpf - 9.0 hpf). At 5.0 hpf, *Ci-cdc25* expression was observed at both the anterior and posterior epidermis. At 5.5 hpf, epidermal expression of *Ci-cdc25* was seen. Strong expression of *Ci-cdc25* was observed in the neural plate (bracket). At 6.0 hpf, a distinct signal was observed only in the anterior epidermis. At 6.5 hpf, *Ci-cdc25* was expressed in the epidermis near the anterior pole. At 7.0 hpf, no signal was detected. At 7.5 hpf, the expression of *Ci-cdc25* was detected at the posterior-most epidermis (arrowhead). *Ci-cdc25* was also expressed in the neural plate (np) and mesenchyme (Me). At 8.0 hpf, epidermal expression of *Ci-cdc25* was somewhat expanded toward the anterior region (bracket). At 8.5 - 9.0 hpf, the entire epidermis was weakly stained. Scale bar: 50 μm. (B) Precursor blastomeres of epidermis (a4.2 and b4.2) were isolated at the 8-cell stage and cultured until the time indicated. Relative mRNA level was quantified in the cultured precursors of epidermis at the time when the control embryos are in the gastrula stage (5 hpf) or the neurula stage (7 hpf and 8 hpf). *Ci-EF1α* was used as a normalizer gene. (C) Effect of injecting *Ci-cdc25* MO on the interphase length of epidermal cells. Interphase was defined by the nuclear localized fluorescence of mVenus-PCNA. Average interphase length of epidermal cells at the 9th, 10th and 11th cell cycles (bar) and individual interphase length of three independent embryos (dots) are shown. (D) Effect of injecting *Ci-cdc25* mRNA on the interphase length of epidermal cells. (E) Effect of *Ci-cdc25* mRNA injection on the interphase progression of epidermal cells. The fluorescence of mVenus-PCNA is shown. Late S-phase was recognized by the foci in the nucleus.

Details are given in the main text. Time is indicated hour : min. Bar, 10 μm.

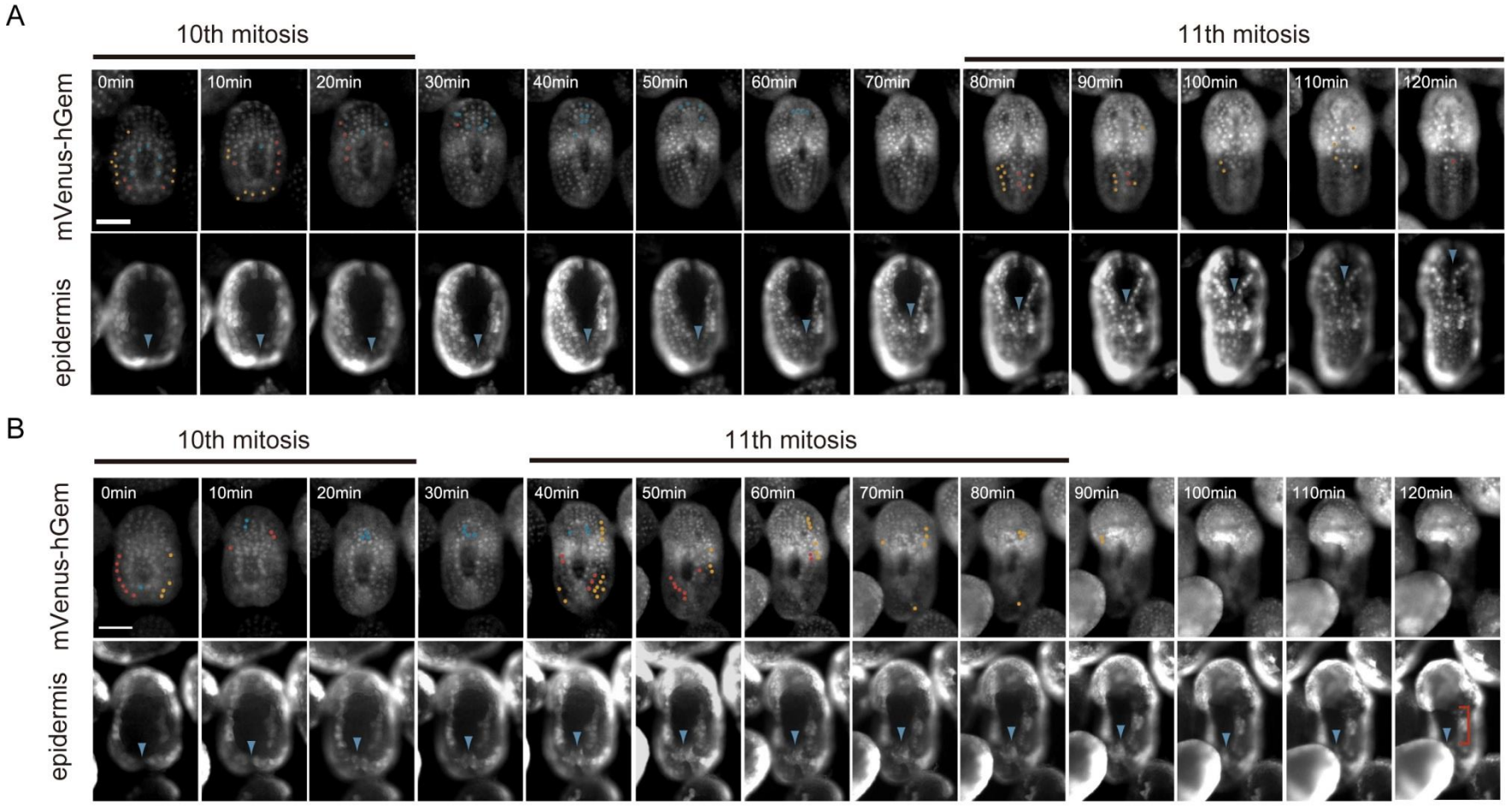
A
10th mitosis
11th mitosis
mVenus-hGem
epidermis
0min
10min
20min
30min
40min
50min
60min
70min
80min
90min
100min
110min
120min
B
10th mitosis
11th mitosis
mVenus-hGem
epidermis
0min
10min
20min
30min
40min
50min
60min
70min
80min
90min
100min
110min
120min

Figure4

Fig. 4. Targeted overexpression of *Ci-cdc25* in the epidermis disrupted neurulation. (A, B) Overexpression of *Ci-cdc25* disrupts the neural tube closure. Time-lapse images of embryos into which mVenus-hGem(1/110) mRNA and pSPCiEpi1GAP43C (control, A), or mVenus-hGem(1/110) and pSPCiEpi1Cicdc25CiEpi1GAP43C (*Ci-cdc25* overexpressed, B), were microinjected. Time-lapse imaging was done at 5-min intervals and from the dorsal side. In this figure, time-lapse images taken at 10-min intervals are shown. The beginning of the 10th mitosis was set as 0 min in each case. Fluorescence of GAP43-CFP fusion (lower column) shows the area covered by the epidermis. Cells that entered into pro-metaphase within the next 5-min interval were marked with dots (red, dorsal midline epidermal cells; orange, other epidermal cells; blue, neural precursor cells). Note that the 11th mitosis started 40 min after the 10th mitosis in the *Ci-cdc25*-overexpressed embryo, while it started at 80 min in the control embryo. In the *Ci-cdc25*-overexpressed embryo, neural tube closure did not occur (a red parenthesis).

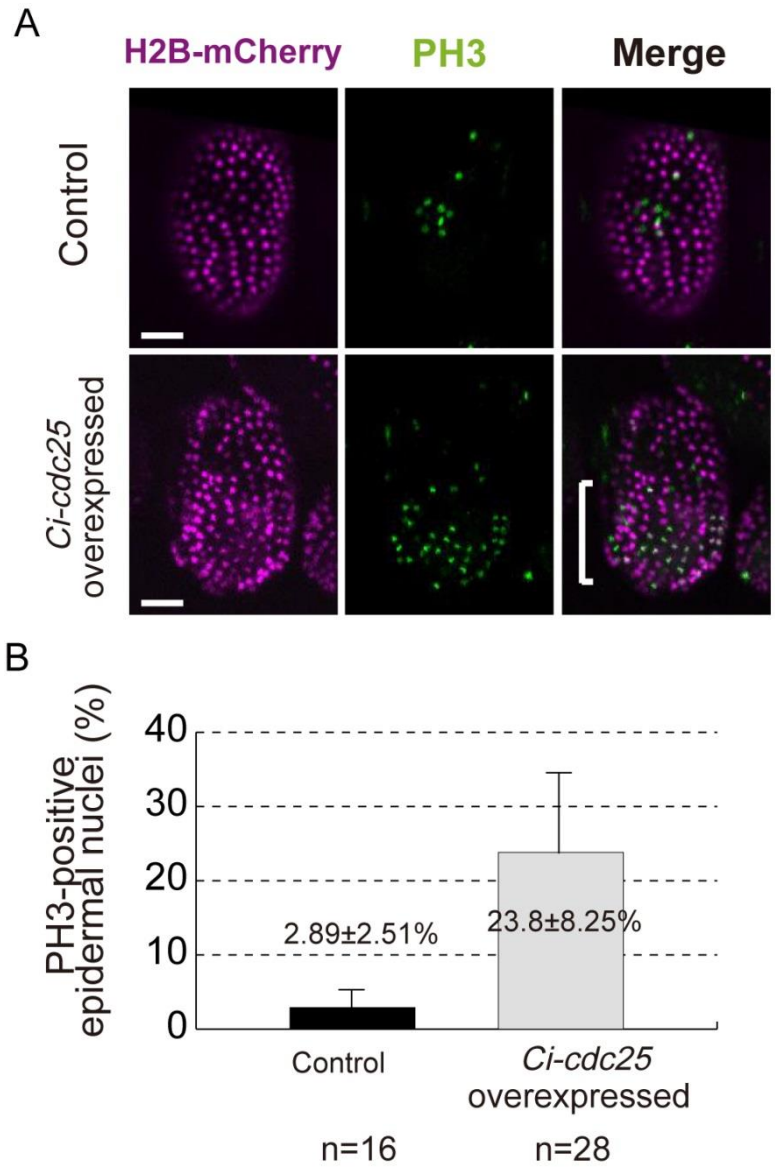
A
H2B-mCherry
PH3
Merge
Control
Ci-cdc25 overexpressed
B
PH3-positive epidermal nuclei (%)
40
30
20
10
0
2.89±2.51%
23.8±8.25%
Control
Ci-cdc25 overexpressed
n=16
n=28

Figure 5

Fig. 5. Epidermis specific overexpression of *Ci-cdc25* induced precocious mitosis during neurulation. (A) Precocious epidermal cell division induced by overexpression of *Ci-cdc25*, which was shown by immunostaining of phospho-histone H3 (PH3). A control embryo at 7.75 hpf, when epidermal cells are in the G2 phase of the 11th cell cycle. Nuclei of epidermal cells were stained with histone H2B-mCherry fusion protein, which was driven by *Ci-EpiI* promoter. PH3 signals are shown in green, and nuclei of epidermal cells are shown in magenta. No epidermal cells showed a PH3 signal. An embryo in which *Ci-cdc25* was overexpressed in the epidermis. Some of the epidermal cells in the tail region (bracket) showed PH3 signals, suggesting that they were in the M phase. (B) The percentage of PH3-positive epidermal cells. Error bars represent standard error.

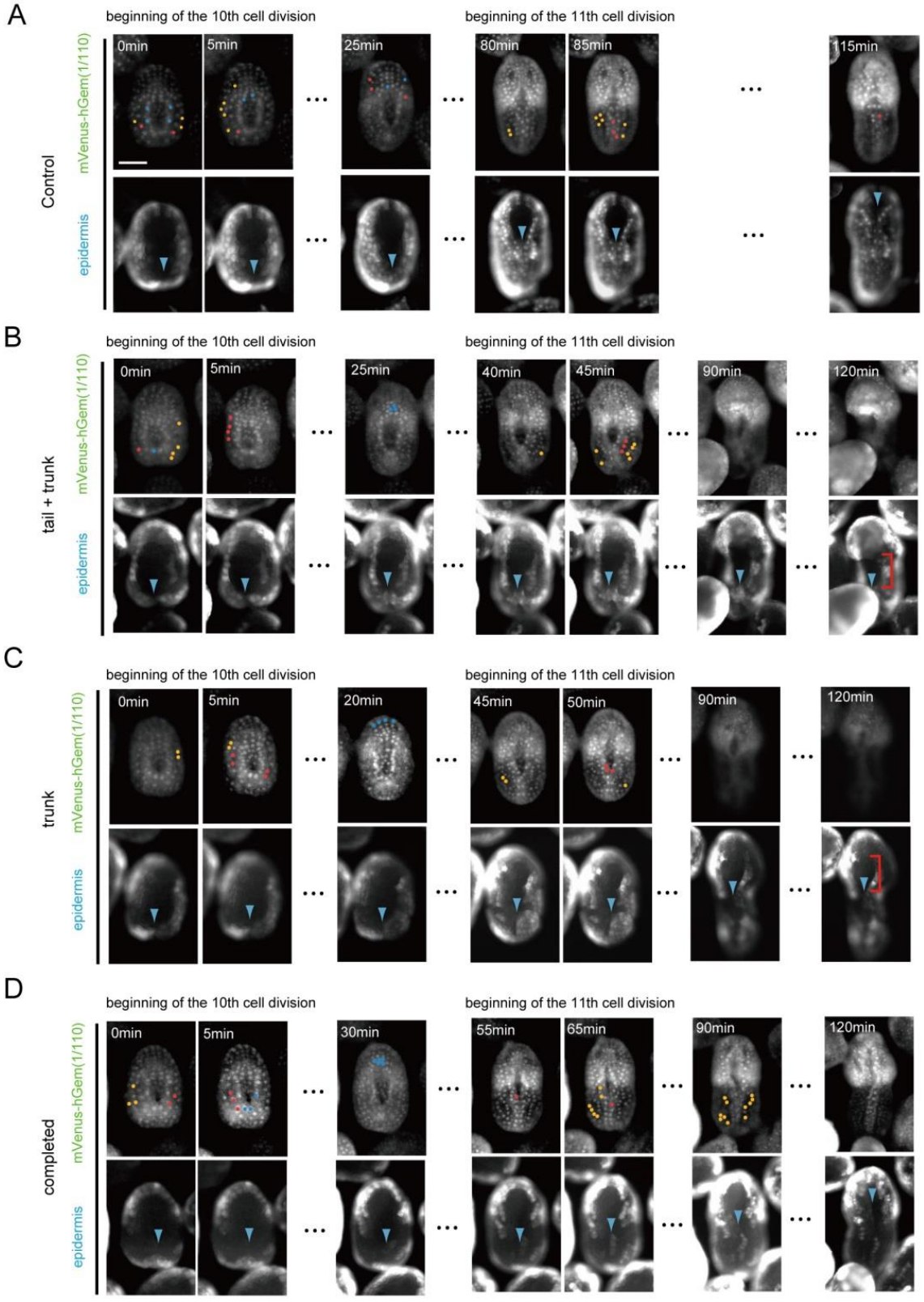
A
beginning of the 10th cell division
beginning of the 11th cell division
Control
mVenus-hGem(1/110)
epidermis
0min
5min
25min
80min
85min
115min
B
beginning of the 10th cell division
beginning of the 11th cell division
tail + trunk
mVenus-hGem(1/110)
epidermis
0min
5min
25min
40min
45min
90min
120min
C
beginning of the 10th cell division
beginning of the 11th cell division
trunk
mVenus-hGem(1/110)
epidermis
0min
5min
20min
45min
50min
90min
120min
D
beginning of the 10th cell division
beginning of the 11th cell division
completed
mVenus-hGem(1/110)
epidermis
0min
5min
30min
55min
65min
90min
120min

Figure 6

Fig. 6. Three types of phenotypes observed in *Ci-cdc25*-overexpressed embryos.
(A) A control embryo into which mVenus-hGem(1/110) and pSPCiEpi1GAP43C were introduced. This embryo completed neural tube closure. (B-D) *Ci-cdc25*-overexpressed embryos into which mVenus-hGem(1/110) and pSPCiEpi1Cicdc25CiEpi1GAP43C were introduced. (B) An embryo whose neural tube closure was severely affected. In this embryo, the neural tube of both the tail and trunk was not closed (bracket). (C) An embryo showing incomplete neural tube closure. In this embryo, the neural tube of the trunk was not closed (bracket). (D) An embryo showing completed neural tube closure. In this embryo, expression of mVenus-hGem(1/110) showed that the 11th mitosis was initiated after neural tube closure.

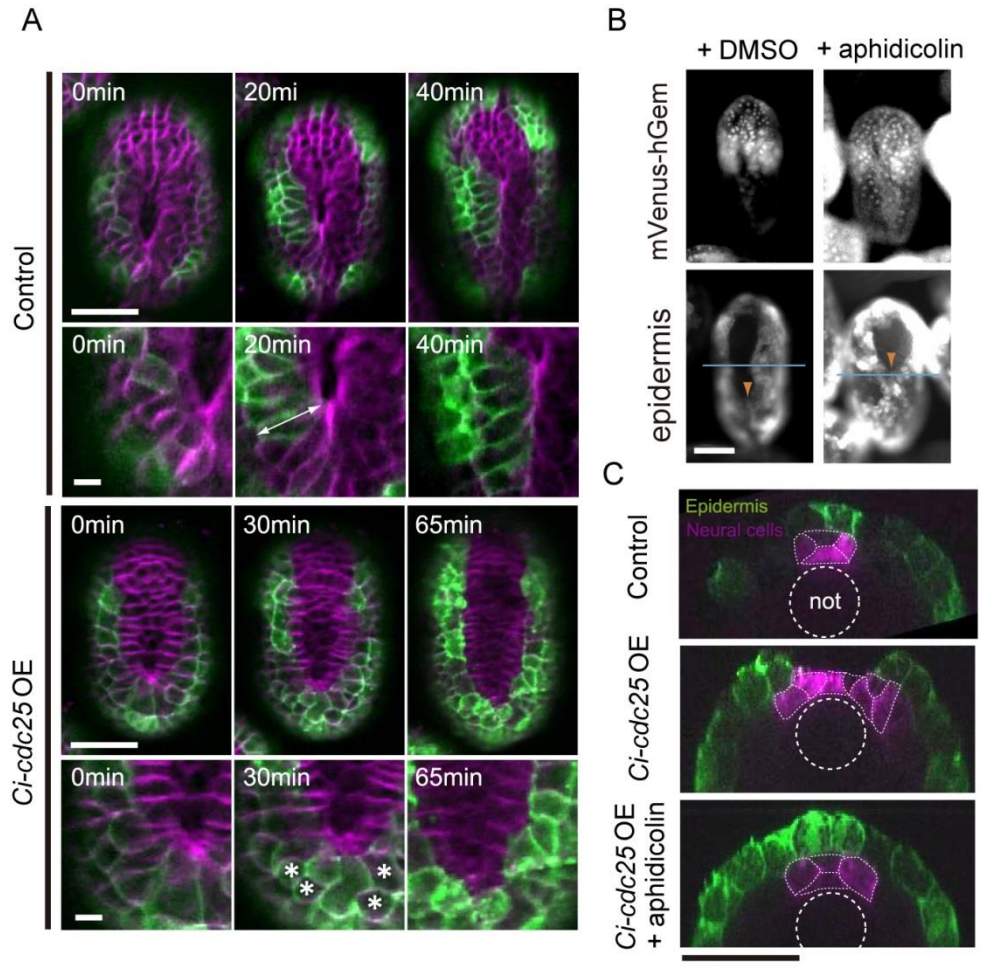
A
Control
0min
20mi
40min
0min
20min
40min
Ci-cdc25 OE
0min
30min
65min
0min
30min
65min
B
+ DMSO
+ aphidicolin
mVenus-hGem
epidermis
C
Control
Epidermis
Neural cells
not
Ci-cdc25 OE
Ci-cdc25 OE
+ aphidicolin

Figure7

Fig. 7. *Ci-cdc25* overexpression disrupts the cell shape changes of epidermal cells during neurulation and inhibits neural tube formation.

(A) Cell shape changes of the epidermal cells during neural tube closure. Single confocal planes are shown of the embryos expressing pSPCiEpi1KCAAX (control) or pSPCiEpi1CiCdc25CiEpi1KCAAX (*Ci-cdc25* overexpressed) that were viewed from the dorsal side. Green signals represent Kaede-CAAX fusion proteins that label plasma membrane of the epidermal cells, and magenta signals represent counterstaining of the plasma membrane of all cells with FM4-64. The control embryo expressed Kaede-CAAX in the left half of the epidermal cells. In the control embryo, the epidermal cells were elongated toward the midline (t = 20 - 40, a doubleheaded arrow). At 40 min, the tail epidermal cells moved toward the midline and the left and right epidermis was fused. In the *Ci-cdc25*-overexpressed embryo (t = 0 - 30), elongation of epidermal cells was not observed, and zippering was not initiated even at 65 min after the 10th mitosis. Instead, some epidermal cells performed the 11th mitosis at 30 min. Two pairs of daughter cells are indicated by asterisks as examples. Bar, 50 μm for the upper column and 10 μm for the lower column. (B) Precocious epidermal cell division induced by overexpression of *Ci-cdc25* inhibited neural tube formation. The plasma membrane of epidermal cells was labeled with Venus-CAAX fusion proteins (green), driven by *Ci-Epi1* promoter. The plasma membrane of neural plate cells was labeled with mCherry-CAAX fusion proteins (magenta), driven by a neural tissue-specific promoter *Ci-ETR*. Three fluorescent cross-sections of the tail region of a control embryo (top), *Ci-cdc25*-overexpressing embryo (middle) and *Ci-cdc25*-overexpressing and aphidicolin-treated embryo (bottom) are shown. Neural cells are outlined with dotted lines. In ascidians, the tail nerve cord is formed from four rows of cells: one dorsally,

one ventrally and two laterally located. Such a formation of the tail nerve cord was seen in the control embryo. In the *Ci-cdc25*-overexpressing embryo, neural cells did not form a tubular structure and they were laterally aligned. A clear nerve cord with four rows of cells was formed in the *Ci-cdc25*-overexpressing and aphidicolin-treated embryo. Scale bar: 50 μm. (C) Aphidicolin treatment reverses the *Ci-cdc25* overexpression effect on neural tube closure. Top row: *Ci-cdc25*-overexpressing control embryos that were treated with DMSO from 7.0 hpf (+DMSO) showed defects in neural tube closure in the tail region, whereas *Ci-cdc25*-overexpressing embryos that were treated with aphidicolin from 7.0 hpf (+Aphidicolin) completed neural tube closure in the tail region. Arrowheads represent the position of the anterior margin of the closed neural tube. Blue lines indicate the boundary between the trunk and tail. Bottom row: Fluorescence of mVenus-hGem(1/110) in the *Ci-cdc25*-overexpressing embryos. In the aphidicolin-treated embryos, some epidermal cells showed nuclear localization of mVenushGem(1/110), suggesting that their cell cycle progression was arrested. Scale bar: 50 μm.

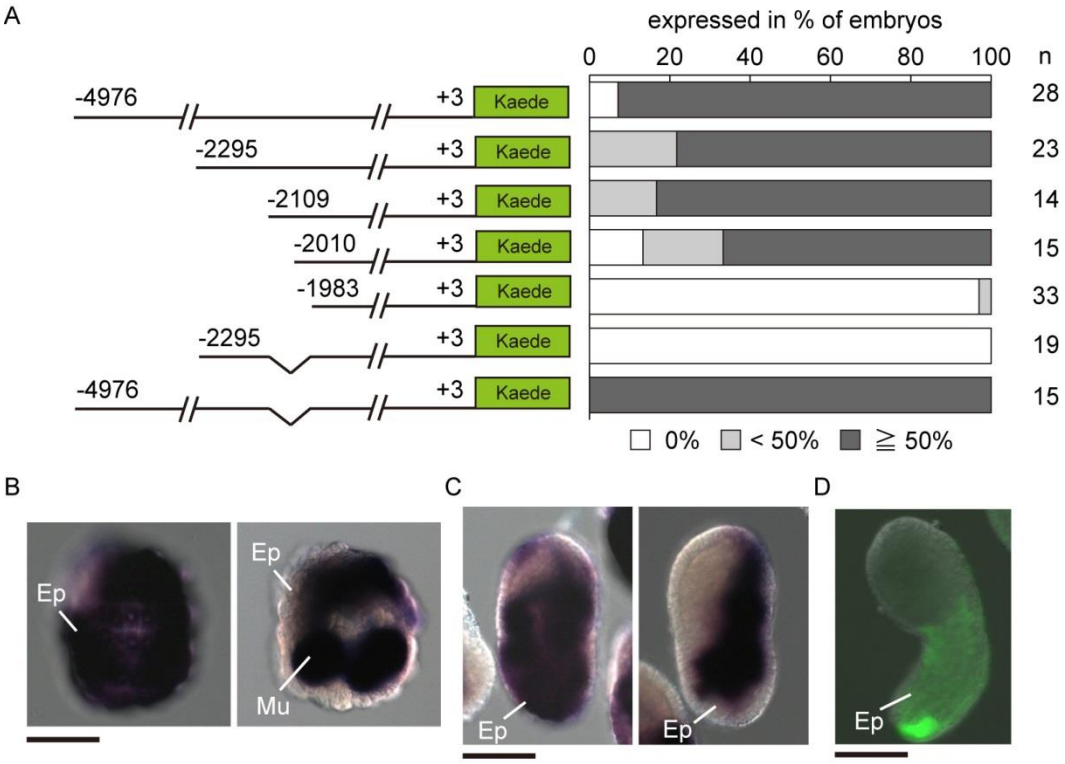
A
expressed in % of embryos
0
20
40
60
80
100
n
-4976
+3
Kaede
28
-2295
+3
Kaede
23
-2109
+3
Kaede
14
-2010
+3
Kaede
15
-1983
+3
Kaede
33
-2295
+3
Kaede
19
-4976
+3
Kaede
15
0%
< 50%
≧ 50%
B
Ep
Ep
Mu
C
Ep
Ep
D
Ep

Figure 8

Fig. 8. Isolation of epidermal enhancer from the upstream regulatory region of *Ci-cdc25*. (A) Deletion analysis of *Ci-cdc25* upstream region. Embryos were electroporated with various deletion constructs shown on the left. The reporter *Kaede* expression was detected by *in situ* hybridization. The right graph shows the percentage of embryos expressing *Kaede* expression in 0 %, within 50 % and over 50 % of the epidermal territory. (B-C) The embryo expressing the construct *pcdc25*(2295 bp)-*Kaede* (left) or *pcdc25*(2295 bp, Δ1988-2110)-*Kaede* (right). *Kaede* mRNA was detected by *in situ* hybridization at the gastrula stage (B, 5.5 hpf, ventral view) and at the tailbud stage (C, 8.5 hpf, lateral view) respectively. Note that reporter expression was lost from the epidermis (Ep). muscle; Mu, Bar, 50 μm. (D) The embryo expressing the construct in which *cis*-regulatory sequence between upstream 1988 bp and 2110 bp was placed at the upstream of forkhead basal promoter. Kaede fluorescence was detected in the epidermis (Ep). Bar, 50 μm.

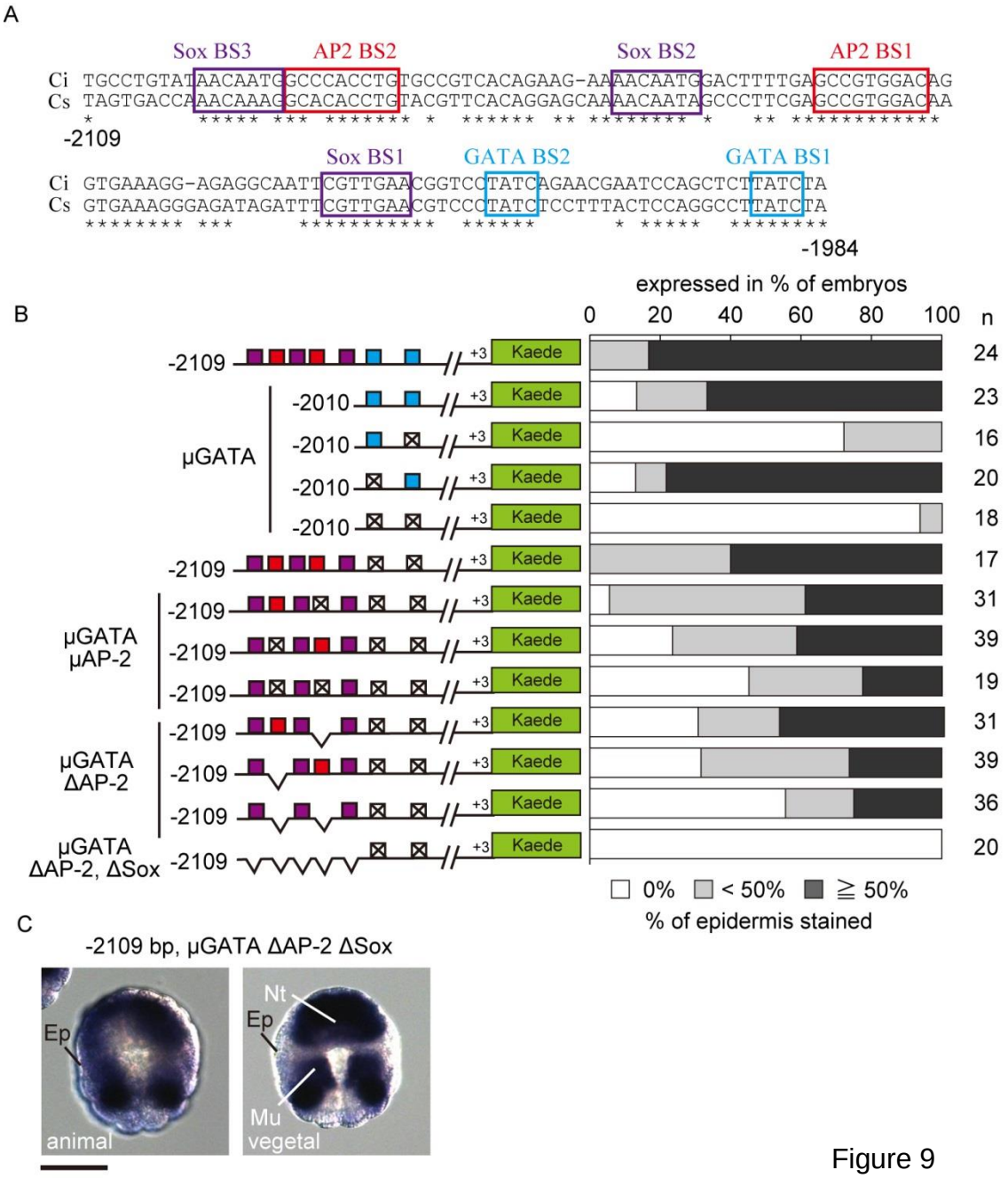
A
Sox BS3
AP2 BS2
Sox BS2
AP2 BS1
Ci TGCCTGTATAACAATGGCCCACCTGTGCCGTCACAGAAG-AAAACAATGGACTTTTGAGCCGTGGACAG
Cs TAGTGACCAAACAAAGGCACACCTGTACGTTCACAGGAGCAAAACAATAGCCCTTCGAGCCGTGGACAA
-2109
Sox BS1
GATA BS2
GATA BS1
Ci GTGAAAGG-AGAGGCAATTCGTTGAACGGTCCTATCAGAACGAATCCAGCTCTTATCTA
Cs GTGAAAGGGAGATAGATTTCGTTGAACGTCCCTATCTCCTTTACTCCAGGCCTTATCTA
-1984
B
expressed in % of embryos
0
20
40
60
80
100
n
-2109
+3
Kaede
24
μGATA
-2010
23
16
20
18
μGATA
μAP-2
17
31
39
19
μGATA
ΔAP-2
31
39
36
μGATA
ΔAP-2, ΔSox
20
0%
< 50%
≧ 50%
% of epidermis stained
C
-2109 bp, μGATA ΔAP-2 ΔSox
Ep
animal
Nt
Ep
Mu
vegetal

Figure 9

Fig. 9. The epidermal enhancer of *Ci-cdc25* is synergistically activated by the GATA, AP-2 and Sox binding sites. (A) Phylogenetic footprinting of the epidermal enhancer of *Ciona intestinalis* (Ci) *cdc25* and the corresponding sequence from *Ciona savigni* (Cs) genome. The boxed sequences represent the putative binding sites for AP-2, GATA and Sox transcription factors. (B) Mutation or deletion in the putative GATA, AP-2 and Sox binding sites resulted in the reduction of epidermal expression of *Kaede* reporter. Embryos were electroporated with various constructs carrying mutation or deletion in the epidermal enhancer as schematized on the left. The bar graph on the right shows the percentage of the embryos expressing *Kaede* expression in 0%, within 50% and over 50% of the epidermal territory. (C) The embryo expressing the construct *pcdc25*(2109 bp)-*Kaede* in which two putative GATA binding sites were mutated, two putative AP-2 binding sites were deleted and three putative Sox binding sites were deleted. The expression of *Kaede* was detected using *in situ* hybridization on *Kaede* mRNA. Note that although the expression of *Kaede* in the epidermis (Ep) is significantly reduced, in the notochord (Nt) and the muscle (Mu) was retained.

A
Ci-IF-C
Ci-IF-D
Control
Ci-AP2L2 MO
Ci-AP2L2 MO
+ Ci-AP2L2
En-AP2L2
B
Ci-IF-C
Ci-IF-D
Control
En-Ci-GATA-a
En-Ci-GATAa
+ Ci-AP2L2
C
Ci-Epi1
Control
Ci-AP2L2 MO
En-AP2L2
En-Ci-GATA-a
En-Ci-GATAa
+ Ci-AP2L2
D
Ci-Epi1
DMSO
1-azakenpaullone
1-azakenpaullone
+ Ci-AP2L2

Figure10

Fig. 10. *Ci-AP2L2* directs the differentiation of epidermis at the downstream of Ci-GATA-a (A) The expression of genes encoding the *Ciona* orthologue of keratin pair *Ci-IF-C* and *Ci-IF-D* was examined by *in situ* hybridization. In embryos knocked down with *Ci-AP-2-like2* (*Ci-AP2L2*), the expression of *Ci-IF-C* and *Ci-IF-D* was reduced. The expression of these genes was rescued by co-injection of *Ci-AP2L2* mRNA. Repressor version of *Ci-AP2L2* (*En-Ci-AP2L2*) also inhibited the expression of *Ci-IF-C* and *Ci-IF-D*. (B) *En-Ci-GATA-a* mRNA injection resulted in the inhibition of *Ci-IF-C* and *Ci-IF-D* expression, which could be reversed by co-injecting *Ci-AP2L2* mRNA. (C) Either injection of *Ci-AP2L2* MO or *En-Ci-AP2L2* did not affect the expression of *Ci-Epi1* in the epidermis. *En-Ci-GATA-a* mRNA injection resulted in the inhibition of *Ci-Epi1* expression, which could be reversed by co-injecting *Ci-AP2L2* mRNA. (D) Treatment of embryos with 1-azakenpaullone resulted in the disappearance of *Ci-Epi1* expression. In embryos injected with *Ci-AP2L2* mRNA, the expression of *Ci-Epi1* was observed even the embryos were treated with 1-azakenpaullone. Bar, 50 μm.

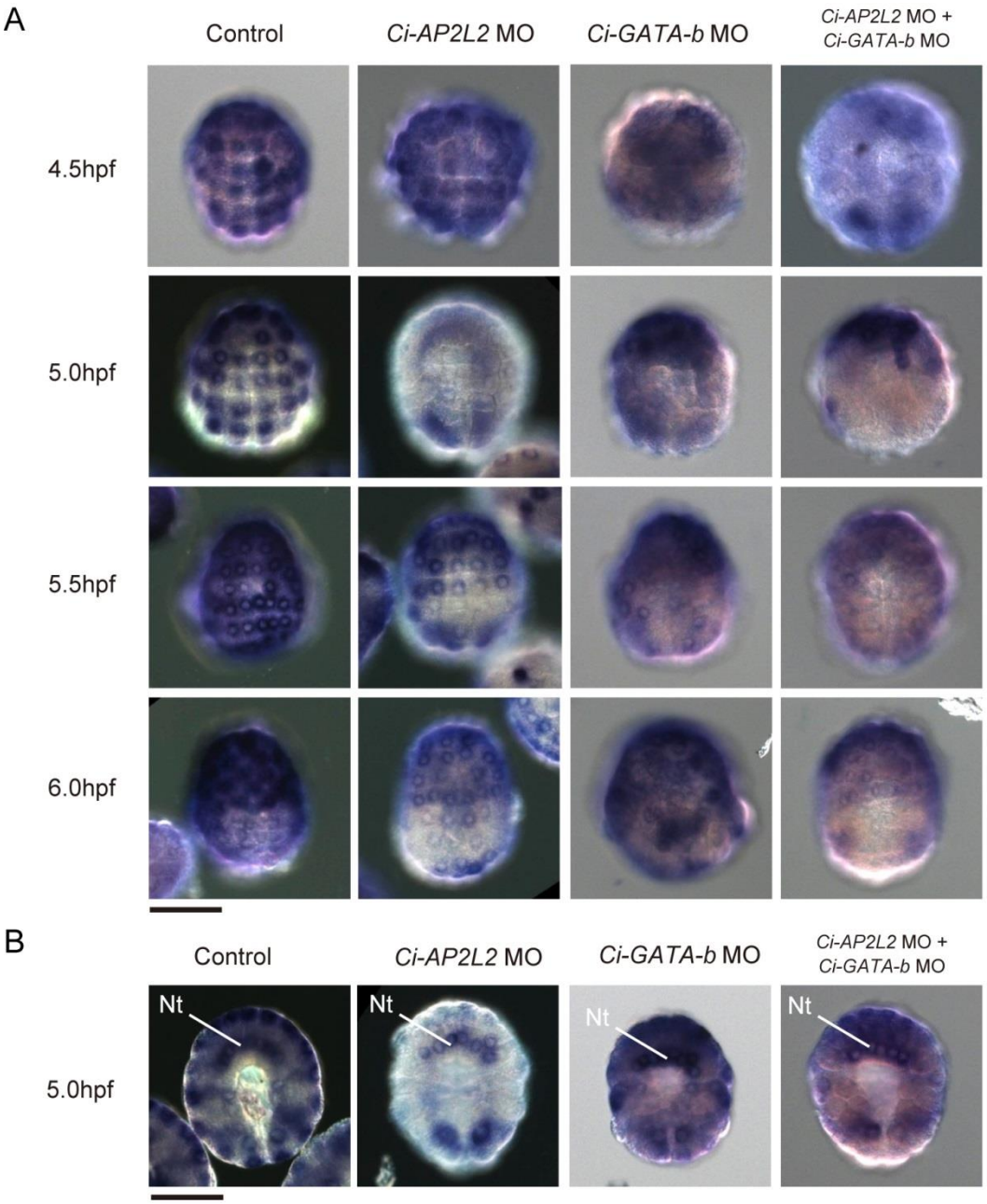
A
Control
Ci-AP2L2 MO
Ci-GATA-b MO
Ci-AP2L2 MO +
Ci-GATA-b MO
4.5hpf
5.0hpf
5.5hpf
6.0hpf
B
Control
Ci-AP2L2 MO
Ci-GATA-b MO
Ci-AP2L2 MO +
Ci-GATA-b MO
5.0hpf
Nt
Nt
Nt
Nt

Figure 11

Fig. 11. *Ci-AP2L2* and *Ci-GATA-b* synergistically activate the epidermal expression of *Ci-cdc25* at the gastrula stage. (A) *Ci-AP2L2* MO injection resulted in the reduction of *Ci-cdc25* expression in the epidermis at 5.0hpf, 5.5hpf while the weaker effect was observed at 6.0hpf. *Ci-GATA-b* MO injection resulted in the reduction of *Ci-cdc25* expression in the epidermis at 4.5hpf, 5.0hpf and 5.5hpf. Co-injection of *Ci-AP2L2* MO and *Ci-GATA-b* MO resulted in the further reduction of *Ci-cdc25* expression in the epidermis at 4.5hpf, 5.0hpf, 5.5hpf and 6.0hpf. Bar, 50 μm. (B) Expression of *Ci-cdc25* in the notochord (Nt) was not affected in the embryos injected with either or *Ci-AP2L2* MO and *Ci-GATA-b* MO or both of them. Bar, 50 μm.

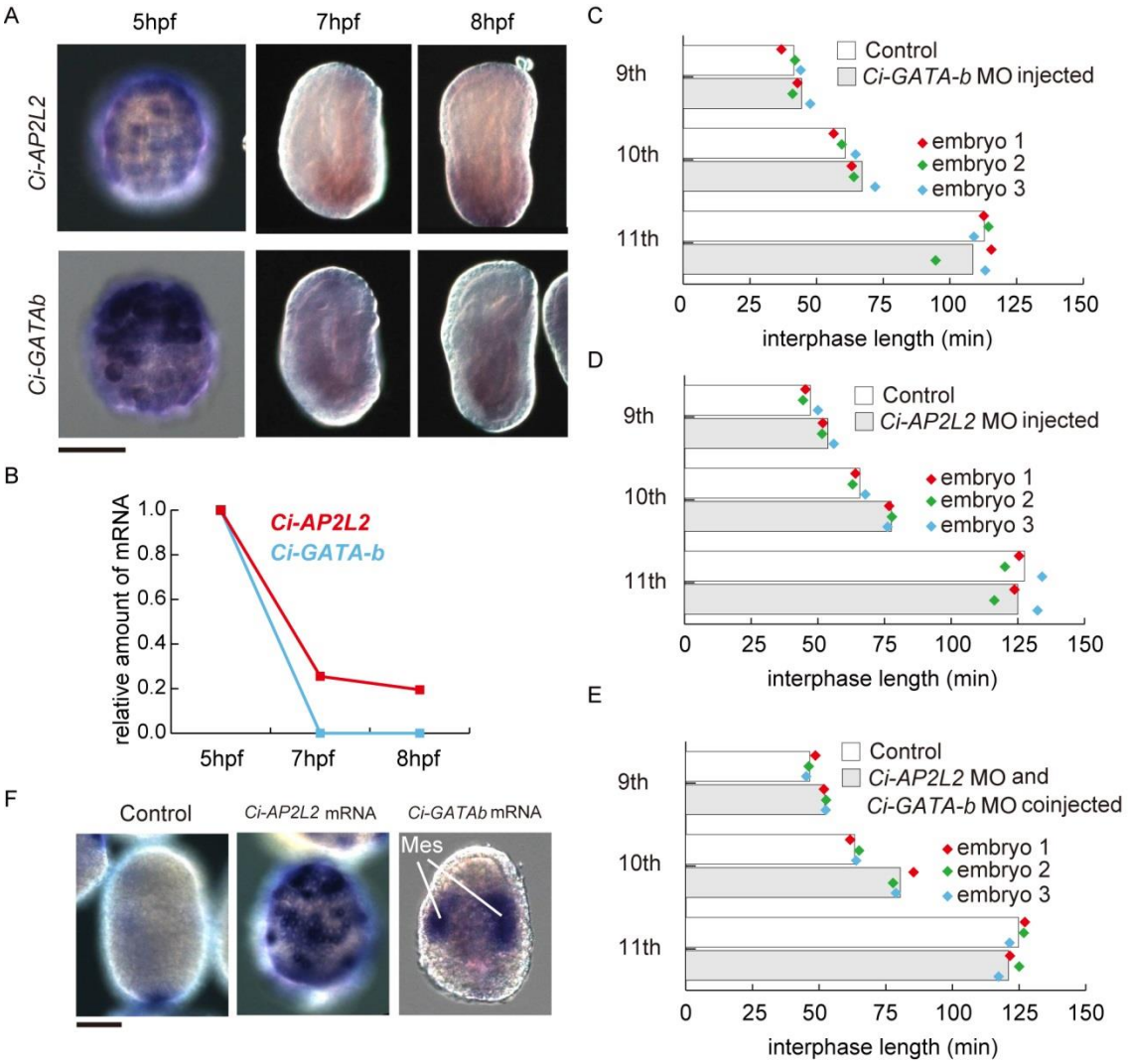
A
5hpf
7hpf
8hpf
Ci-AP2L2
Ci-GATAb
B
relative amount of mRNA
1.0
0.8
0.6
0.4
0.2
0.0
Ci-AP2L2
Ci-GATA-b
5hpf
7hpf
8hpf
C
9th
10th
11th
Control
Ci-GATA-b MO injected
embryo 1
embryo 2
embryo 3
0
25
50
75
100
125
150
interphase length (min)
D
9th
10th
11th
Control
Ci-AP2L2 MO injected
embryo 1
embryo 2
embryo 3
0
25
50
75
100
125
150
interphase length (min)
E
9th
10th
11th
Control
Ci-AP2L2 MO and
Ci-GATA-b MO coinjected
embryo 1
embryo 2
embryo 3
0
25
50
75
100
125
150
interphase length (min)
F
Control
Ci-AP2L2 mRNA
Ci-GATAb mRNA
Mes

Figure 12

Fig. 12. Disruption of zygotic *Ci-AP2L2* and *Ci-GATA-b* expression caused cell cycle lengthening of epidermal cells before neurulatoin. (A) The expression of *Ci-AP2L2* and *Ci-GATA-b* were detected using *in situ* hybridization, at the gastrula stage (5hpf), at the neurula stage (7hpf and 8hpf). Bar, 50 μm. (B) Relative mount of *Ci-AP2L2* mRNA and *Ci-GATA-b* mRNA in the whole embryo at the time when the normal embryos are in gastrula stage (5hpf), at the onset of neurulation (7hpf) and during neurulation (8hpf). (C) Effect of injecting *Ci-AP2L2* mRNA and *Ci-GATA-b* mRNA on the expression of *Ci-cdc25* in the epidermis. Expression of *Ci-cdc25* was examined by *in situ* hybridization at the onset of neurulation (7.0hpf) when *Ci-cdc25* expression is extinguished in the epidermis in wild-type embryos. Expression in the mesenchyme (Mes) is indicated. (D-E) Effects of injecting *Ci-AP2L2* MO, *Ci-GATA-b* MO and co-injection of both on the interphase length of epidermal cells in the 9th, 10th and 11th cell cycle of epidermal cells. Interphase was approximately defined by the nuclear localized fluorescence of mVenus-PCNA. Average interphase length of epidermal cells at the 9th, 10th and 11th cell cycles (bar) and individual average interphase length of three independent embryos (dots) are shown. (F) Effect of injecting *Ci-AP2L2* mRNA or *Ci-GATA-b* mRNA on the epidermal expression of *Ci-cdc25*. Bar, 50 μm.

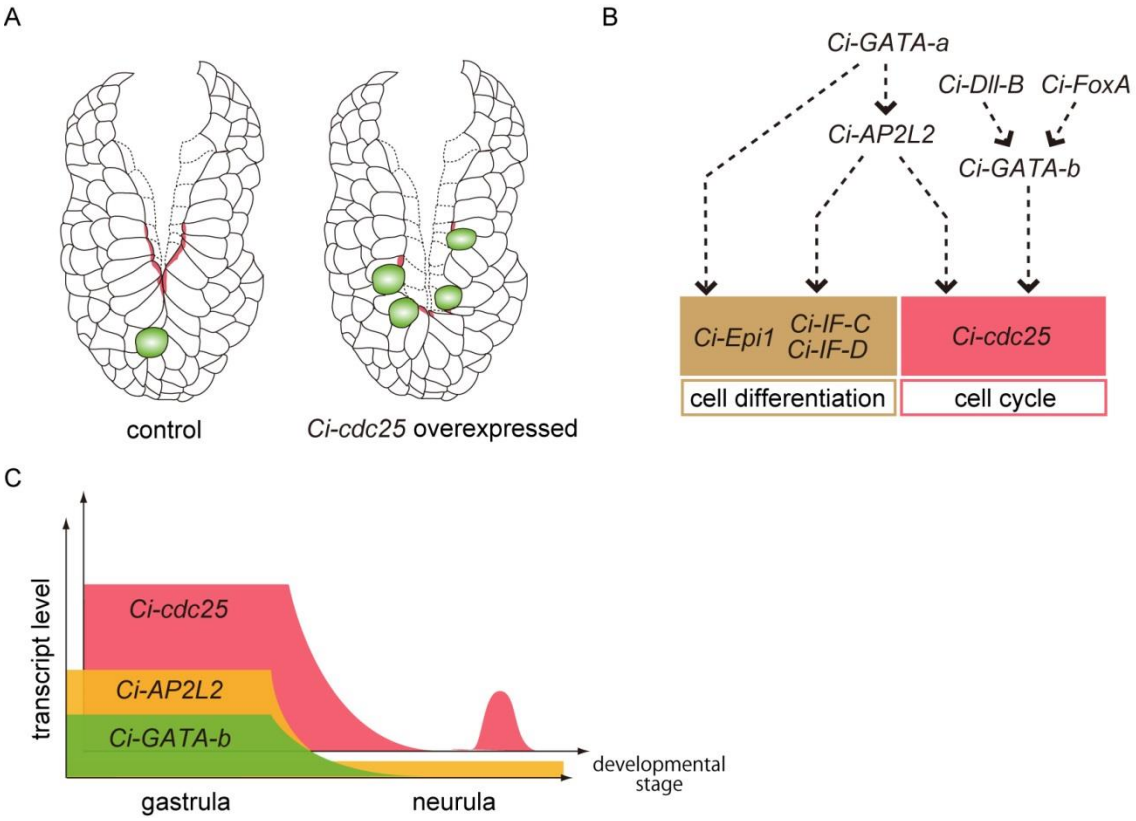
A
control
Ci-cdc25 overexpressed
B
Ci-GATA-a
Ci-Dll-B
Ci-FoxA
Ci-AP2L2
Ci-GATA-b
Ci-Epi1
Ci-IF-C
Ci-IF-D
Ci-cdc25
cell differentiation
cell cycle
C
transcript level
Ci-cdc25
Ci-AP2L2
Ci-GATA-b
developmental stage
gastrula
neurula

Figure 13

Fig. 13. A model for the cell cycle regulation of epidermal cells during neurulation in *Ciona*. (A) Coordination of mitosis and cell movement of the epidermal cells is achieved by lengthening of the interphase. In the control embryos, mitoses of the epidermal cells occur after the completion of neurulation. On the other hand, in the embryos overexpressed with *Ci-cdc25*, F-actin accumulation at the leading edge of the epidermal cells undergoing mitosis was disrupted. Cell movement of the epidermal cells toward the dorsal midline was inhibited, resulting in the failure of neurulation. Red, F-actin; Green, cells in mitosis. (B) Proposed regulatory relationships among *Ci-cdc25*, *Ci-AP2L2* and *Ci-GATA-b* in the control of cell differentiation and cell cycle of epidermal cells. *Ci-AP2L2* directs the differentiation of epidermis by activating the expression of *Ci-IF-C*, *Ci-IF-D* and possibly *Ci-Epi1* at the downstream of *Ci-GATA-a*. *Ci-AP2L2* also regulates the cell cycle of epidermal cells in cooperation with *Ci-GATA-b* by activating the transcription of *Ci-cdc25* in the epidermis at the gastrula stage. Regulation of *Ci-GATA-b* by *Ci-Dll-B* and *Ci-FoxA* was previously reported (Imai et al., 2006). (C) The expression of *Ci-cdc25* in the epidermis declines when embryogenesis progress from the gastrula stage to the neurula stage. The coincident down-regulation of transcription factors *Ci-AP2L2* and *Ci-GATA-b* is observed. Down-regulation of *Ci-AP2L2* and *Ci-GATA-b* at the gastrula-neurula boundary facilitates the interphase lengthening of epidermal cells.

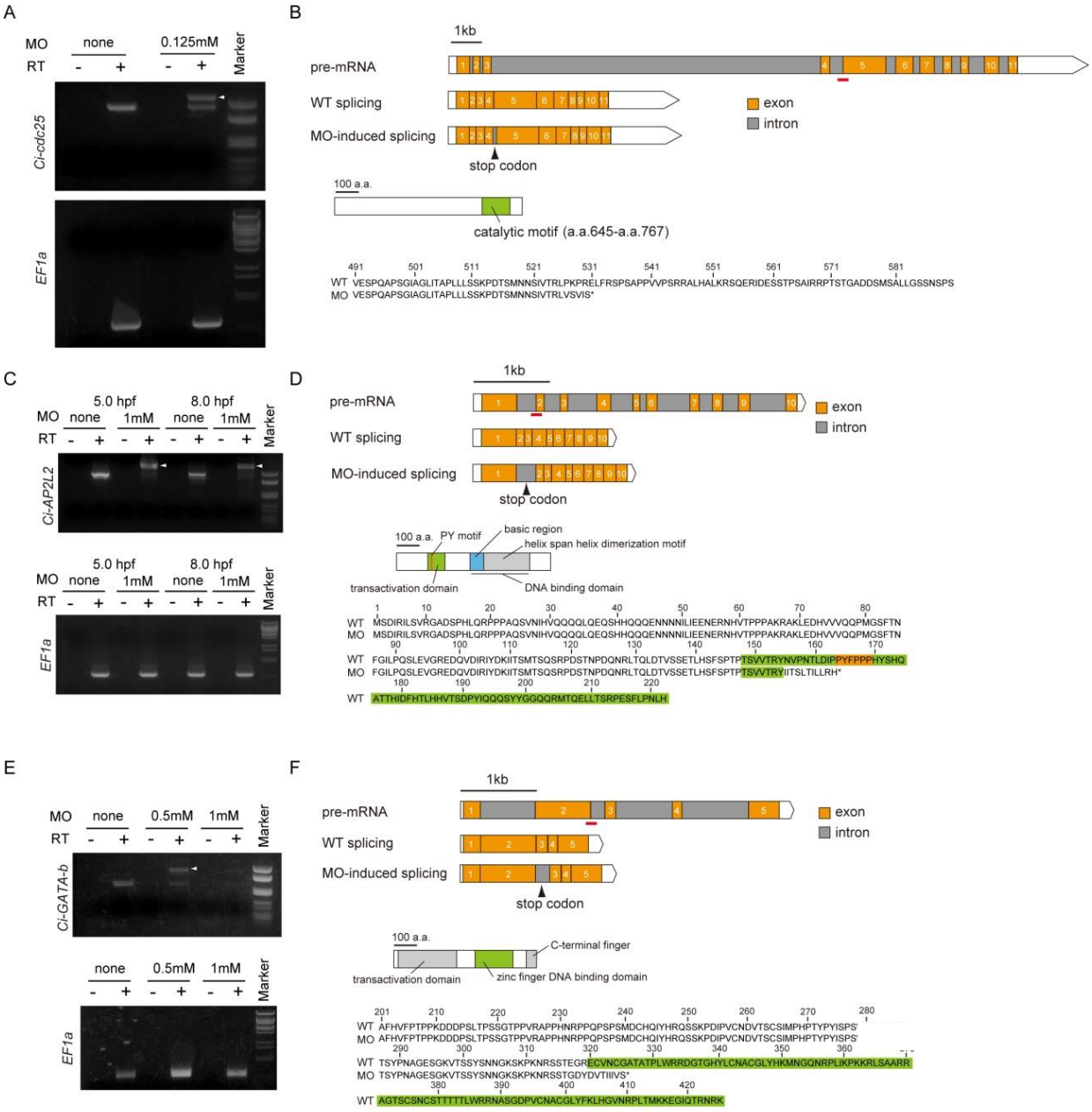
A
MO
none
0.125mM
RT
Marker
Ci-cdc25
EF1a
B
1kb
pre-mRNA
WT splicing
MO-induced splicing
exon
intron
stop codon
100 a.a.
catalytic motif (a.a.645-a.a.767)
WT VESPQAPSGIAGLITAPLLLSSKPDTSMNNSIVTRLPKPRELFRSPSAPPVVPSRRALHALKRSQERIDESSTPSAIRRPTSTGADDSMSALLGSSNSPS
MO VESPQAPSGIAGLITAPLLLSSKPDTSMNNSIVTRLVSVIS*
C
5.0 hpf
8.0 hpf
none
1mM
Ci-AP2L2
EF1a
D
PY motif
basic region
helix span helix dimerization motif
transactivation domain
DNA binding domain
WT MSDIRILSVRGADSPHLQRPPPAQSVNIHVQQQQLQEQSHHQQQENNNNILIEENERNHVTPPPAKRAKLEDHVVVQQPMGSFTN
MO MSDIRILSVRGADSPHLQRPPPAQSVNIHVQQQQLQEQSHHQQQENNNNILIEENERNHVTPPPAKRAKLEDHVVVQQPMGSFTN
WT FGILPQSLEVGREDQVDIRIYDKIITSMTSQSRPDSTNPDQNRLTQLDTVSSETLHSFSPTPTSVVTRYNVPNTLDIPPYFPPPHYSHQ
MO FGILPQSLEVGREDQVDIRIYDKIITSMTSQSRPDSTNPDQNRLTQLDTVSSETLHSFSPTPTSVVTRYIITSLTILLRH*
WT ATTHIDFHTLHHVTSDPYIQQQSYYGGQQRMTQELLTSRPESFLPNLH
E
0.5mM
1mM
Ci-GATA-b
EF1a
F
C-terminal finger
transactivation domain
zinc finger DNA binding domain
WT AFHVFPTPPKDDDPSLTPSSGTPPVRAPPHNRPPQPSPSMDCHQIYHRQSSKPDIPVCNDVTSCSIMPHPTYPYISPS'
MO AFHVFPTPPKDDDPSLTPSSGTPPVRAPPHNRPPQPSPSMDCHQIYHRQSSKPDIPVCNDVTSCSIMPHPTYPYISPS'
WT TSYPNAGESGKVTSSYSNNGKSKPKNRSSTEGRECVNCGATATPLWRRDGTGHYLCNACGLYHKMNGQNRPLIKPKKRLSAARR
MO TSYPNAGESGKVTSSYSNNGKSKPKNRSSTGDYDVTIIIVS*
WT AGTSCSNCSTTTTTLWRRNASGDPVCNACGLYFKLHGVNRPLTMKKEGIQTRNRK

Figure14

Fig. 14. Effect of antisense MOs against *Ci-cdc25*, *Ci-AP2L2* and *Ci-GATA-b*.

(A) Injection of the splice MO against *Ci-cdc25* resulted in disruption of the splicing. Reverse transcriptional (RT)-PCR was performed using the cDNA extracted from the embryos at the tailbud stage (8.5hpf) injected with *Ci-cdc25* MO. The abnormal transcript is indicated by an arrowhead. The bottom column shows the RT-PCR of *Ci-EF1α* (positive control). (B) Sequencing of the abnormal transcript revealed that the 4th intron was not spliced. As a result, a premature stop codon was introduced upstream of the sequence encoding the catalytic motif. The lower amino acid sequence represents the predicted amino acid sequence of the protein translated from the abnormal transcript. Note that the protein is truncated before the catalytic motif. a.a., amino acids. (C) Injection of the splice MO against *Ci-AP2L2* resulted in disruption of the splicing. RT-PCR was performed using the cDNA extracted from the embryos at the gastrula stage (5hpf) and the neurula stage (8hpf) injected with *Ci-AP2L2* MO. The abnormal transcript is indicated by an arrowhead. (D) Sequencing of the abnormal transcript revealed that the 1st intron was not spliced. As a result, a premature stop codon was introduced upstream the sequence encoding the PY-motif, the core sequence in transactivation domain of AP-2 transcription factors. The lower amino acid sequence represents the predicted amino acid sequence of the protein translated from the abnormal transcript. Note that the protein is truncated before the PY-motif (Orange). (E) Injection of the splice MO against *Ci-GATA-b* resulted in disruption of the splicing. RT-PCR was performed using the cDNA extracted from the embryos at the gastrula stage (6hpf) injected with *Ci-GATA-b* MO. The abnormal transcript is indicated by an arrowhead. (F) Sequencing of the abnormal transcript revealed that the 2nd intron was not spliced. As a result, a premature stop codon was introduced in the zinc finger DNA

binding domain. The lower amino acid sequence represents the predicted amino acid sequence of the protein translated from the abnormal transcript. Note that the protein is truncated at the beginning of the zinc finger DNA binding domain (Green).

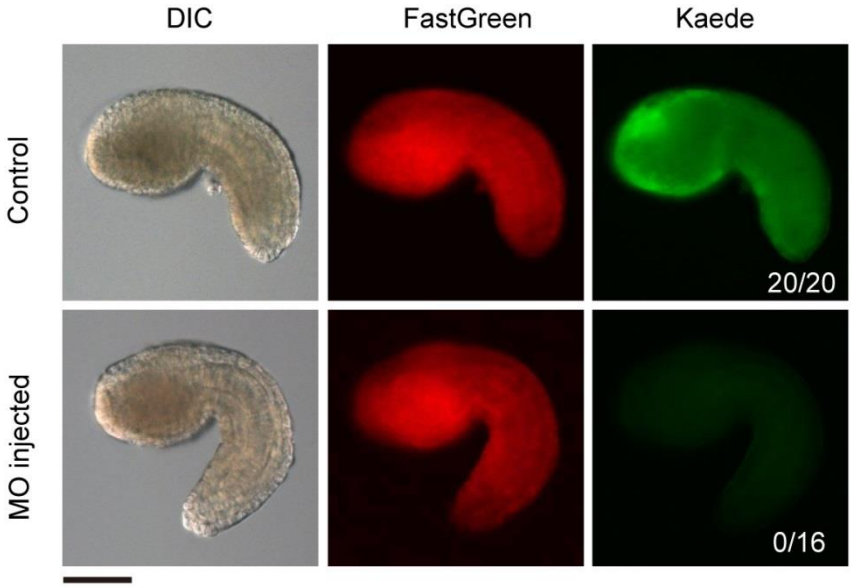

Figure 15

Fig. 15. Effect of antisense MO against *Ci-SoxB1*.

Injection of the ATG MO against *Ci-SoxB1* resulted in the disappearance of Kaede fluorescence. FastGreen dye was used to detect injected solution. The number of embryos expressing Kaede protein in the epidermis is shown at the bottom right. The dominators are total number of embryos examined. Bar, 50 μm.

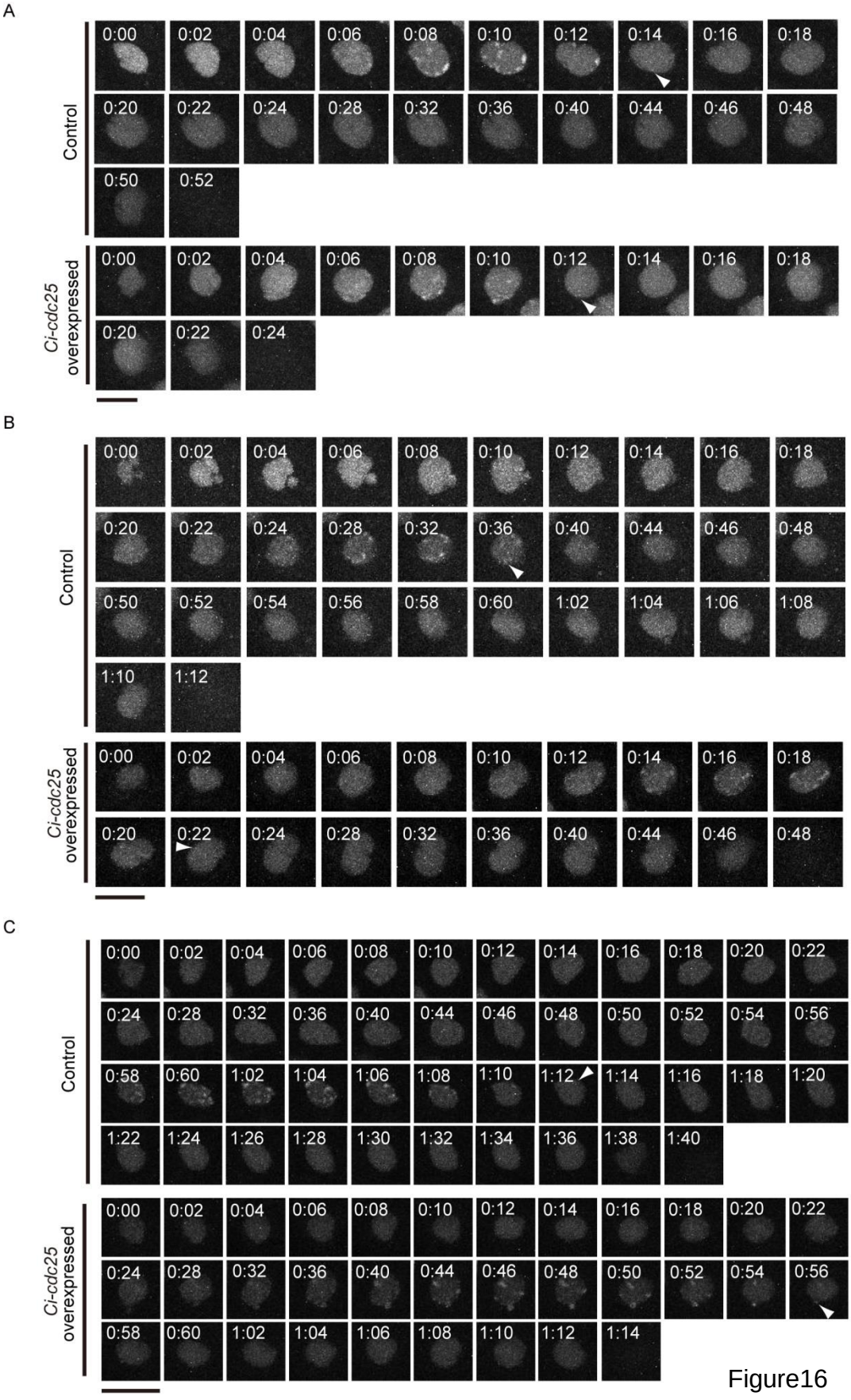
A
Control
0:00
0:02
0:04
0:06
0:08
0:10
0:12
0:14
0:16
0:18
0:20
0:22
0:24
0:28
0:32
0:36
0:40
0:44
0:46
0:48
0:50
0:52
Ci-cdc25 overexpressed
0:00
0:02
0:04
0:06
0:08
0:10
0:12
0:14
0:16
0:18
0:20
0:22
0:24
B
Control
0:00
0:02
0:04
0:06
0:08
0:10
0:12
0:14
0:16
0:18
0:20
0:22
0:24
0:28
0:32
0:36
0:40
0:44
0:46
0:48
0:50
0:52
0:54
0:56
0:58
0:60
1:02
1:04
1:06
1:08
1:10
1:12
Ci-cdc25 overexpressed
0:00
0:02
0:04
0:06
0:08
0:10
0:12
0:14
0:16
0:18
0:20
0:22
0:24
0:28
0:32
0:36
0:40
0:44
0:46
0:48
C
Control
0:00
0:02
0:04
0:06
0:08
0:10
0:12
0:14
0:16
0:18
0:20
0:22
0:24
0:28
0:32
0:36
0:40
0:44
0:46
0:48
0:50
0:52
0:54
0:56
0:58
0:60
1:02
1:04
1:06
1:08
1:10
1:12
1:14
1:16
1:18
1:20
1:22
1:24
1:26
1:28
1:30
1:32
1:34
1:36
1:38
1:40
Ci-cdc25 overexpressed
0:00
0:02
0:04
0:06
0:08
0:10
0:12
0:14
0:16
0:18
0:20
0:22
0:24
0:28
0:32
0:36
0:40
0:44
0:46
0:48
0:50
0:52
0:54
0:56
0:58
0:60
1:02
1:04
1:06
1:08
1:10
1:12
1:14

Figure16

Fig. 16. Effect of *Ci-cdc25* mRNA injection on the interphase progression of epidermal cells. Interphase progression of the 9th epidermal cell cycle (A), 10th epidermal cell cycle (B) and 11th epidermal cell cycle (C) were monitored in the embryos expressing mVenus-PCNA. The embryos were injected with *Ci-cdc25* mRNA into a single blastomere at the 2-cell stage. The arrowhead indicates the characteristic foci observed at the closing minutes of S-phase in each cell cycle. The time is indicated in hour: min. The characteristic foci at the end of S-phase were indicated by arrowhead. Bars, 10 μm.

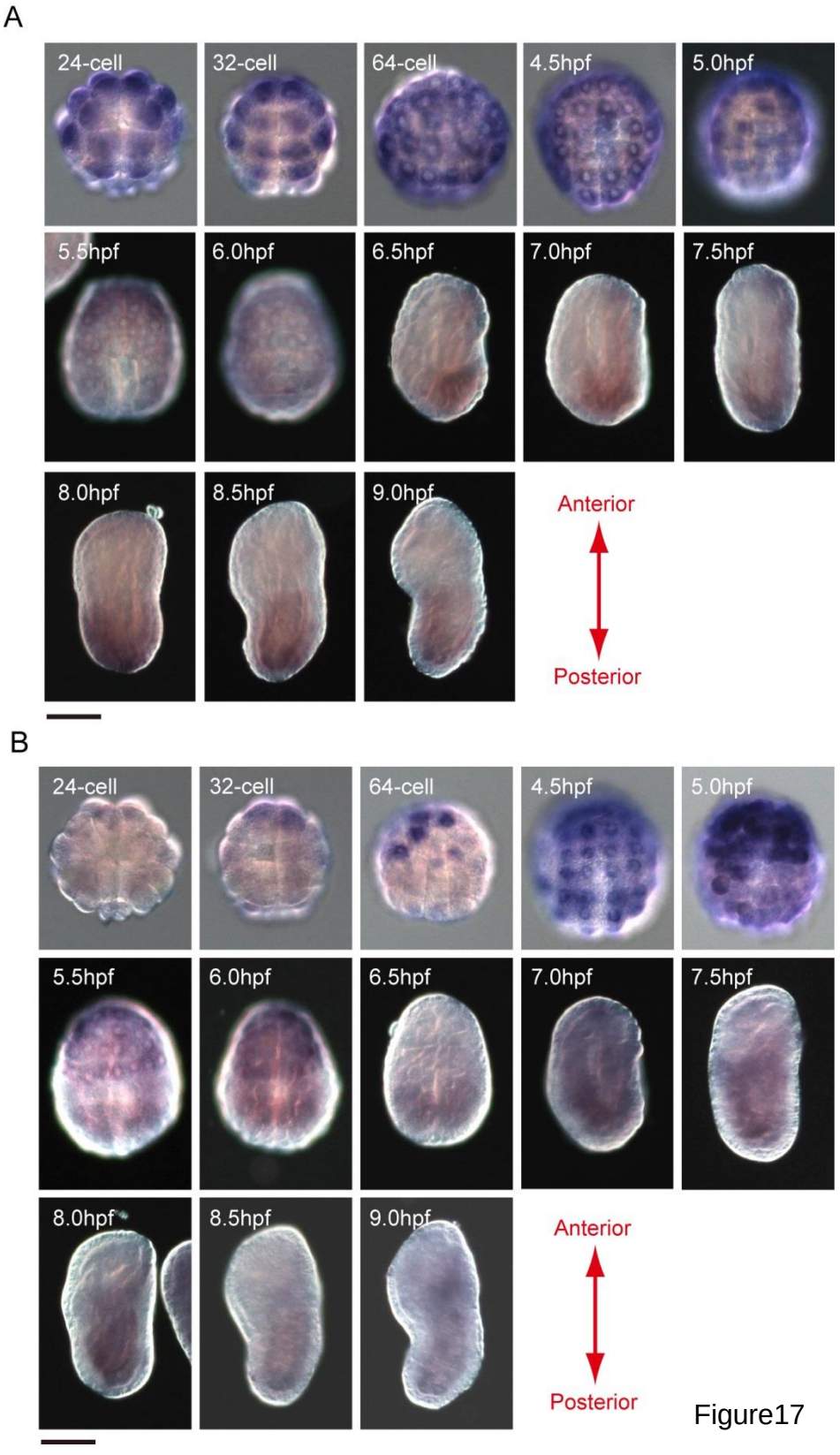
A
24-cell
32-cell
64-cell
4.5hpf
5.0hpf
5.5hpf
6.0hpf
6.5hpf
7.0hpf
7.5hpf
8.0hpf
8.5hpf
9.0hpf
Anterior
Posterior
B
24-cell
32-cell
64-cell
4.5hpf
5.0hpf
5.5hpf
6.0hpf
6.5hpf
7.0hpf
7.5hpf
8.0hpf
8.5hpf
9.0hpf
Anterior
Posterior

Figure17

Fig. 17. Temporal changes in the expression of *Ci-AP2L2* and *Ci-GATA-b*.

The expression of *Ci-AP2L2* and *Ci-GATA-b* was detected using *in situ* hybridization. Embryos were viewed from the ventral side (24-cell to 6.0 hpf) or lateral side (6.5 hpf to 9.0 hpf). (A) Strong expression of *Ci-AP2L2* in the epidermis was observed from the 24-cell stage until 5.5 hpf, while only weak expression of *Ci-AP2L2* in the epidermis was observed from 6.0 hpf until 9.0 hpf. (B) Strong expression of *Ci-GATA-b* in the epidermis was observed from 4.5 hpf until 6.0 hpf, while no signal was detected in the epidermis from 6.5 hpf until 9.0 hpf. Bar, 50 μm.

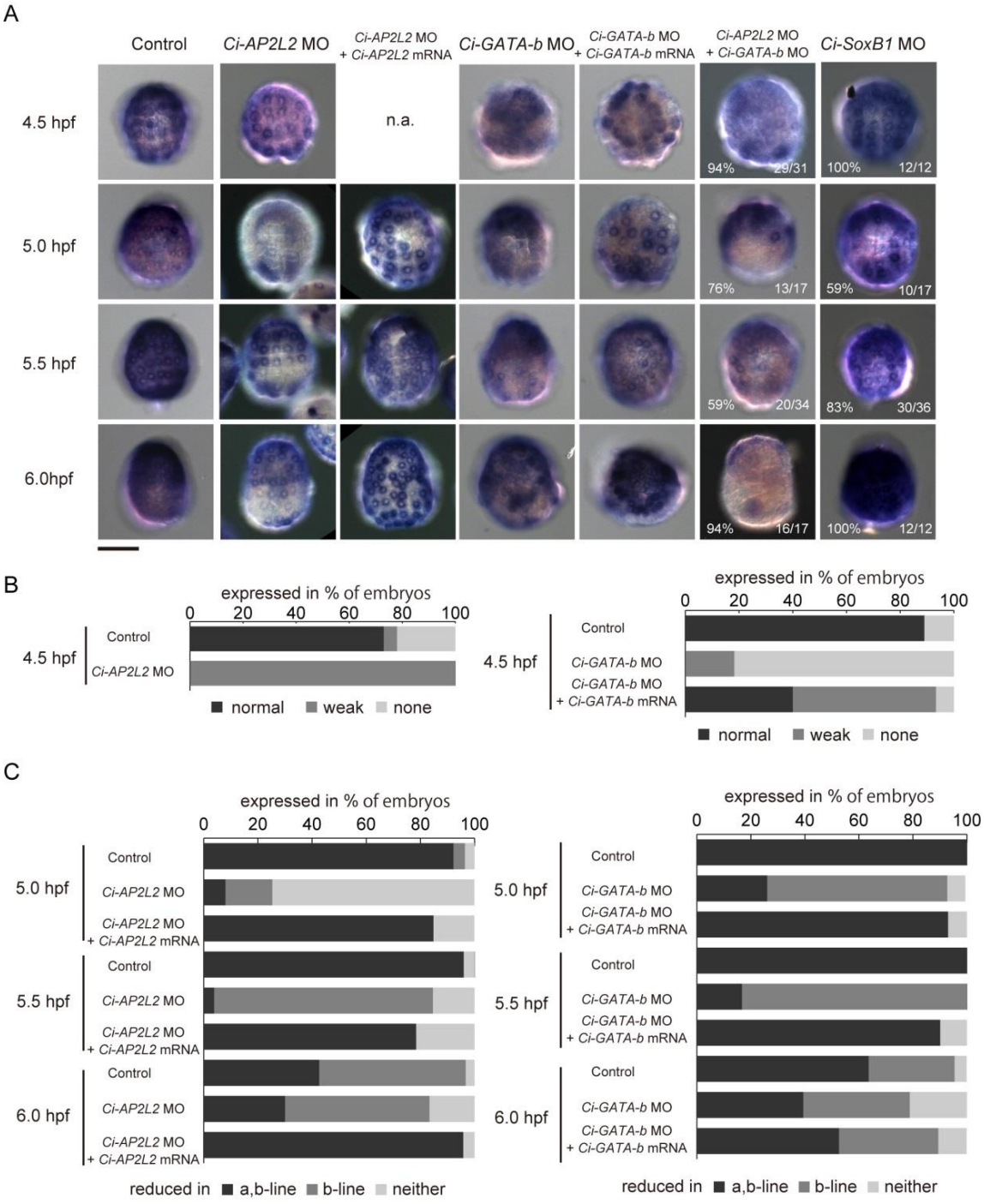
A
Control
Ci-AP2L2 MO
Ci-AP2L2 MO + Ci-AP2L2 mRNA
Ci-GATA-b MO
Ci-GATA-b MO + Ci-GATA-b mRNA
Ci-AP2L2 MO + Ci-GATA-b MO
Ci-SoxB1 MO
4.5 hpf
5.0 hpf
5.5 hpf
6.0hpf
n.a.
94% 29/31
100% 12/12
76% 13/17
59% 10/17
59% 20/34
83% 30/36
94% 16/17
100% 12/12
B
expressed in % of embryos
0 20 40 60 80 100
4.5 hpf
Control
Ci-AP2L2 MO
normal weak none
Ci-GATA-b MO
Ci-GATA-b MO + Ci-GATA-b mRNA
C
5.0 hpf
5.5 hpf
6.0 hpf
Ci-AP2L2 MO + Ci-AP2L2 mRNA
reduced in a,b-line b-line neither
Ci-GATA-b MO + Ci-GATA-b mRNA

Figure18

Fig. 18. *Ci-GATA-b* and *Ci-AP2L2* is necessary and sufficient for the epidermal expression of *Ci-cdc25*. (A) The expression of *Ci-cdc25* was examined by *in situ* hybridization. In the embryos injected with the MOs against *Ci-AP2L2* and *Ci-GATA-b*, epidermal expression of *Ci-cdc25* was reduced. The reduction of *Ci-cdc25* expression in the b-line epidermis was more susceptible to the knock-down of these genes. In the pictures of *Ci-AP2L2* MO + *Ci-GATA-b* MO, the number and percentage of the embryos showed reduced expression of *Ci-cdc25* in the epidermis was shown. In the pictures of *Ci-SoxB1* MO, the number and percentage of the embryos showed normal expression of *Ci-cdc25* in the epidermis was shown. The denominators represent the total number of embryos examined. n.a., not analyzed. Bar, 50 μm. (B) Percentages of embryos expressing *Ci-cdc25* at 4.5 hpf is shown. (C) Percentage of embryos expressing *Ci-cdc25* in the epidermis at 5.0 hpf, 5.5 hpf and 6.0 hpf is shown. Embryos expressing *Ci-cdc25* in the a-line (anterior) and the b-line (posterior) epidermis were counted separately. I found that no embryo shows reduced expression of *Ci-cdc25* exclusively in the a-line epidermis. Bar, 50 μm.

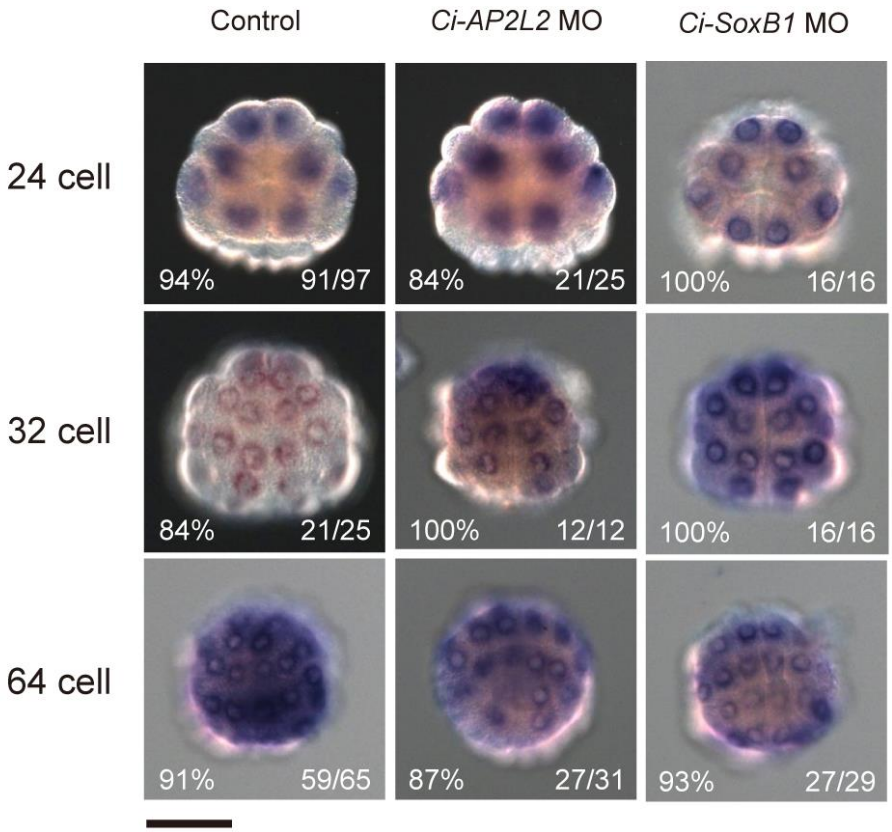
Control
Ci-AP2L2 MO
Ci-SoxB1 MO
24 cell
32 cell
64 cell
94% 91/97
84% 21/25
100% 16/16
84% 21/25
100% 12/12
100% 16/16
91% 59/65
87% 27/31
93% 27/29

Figure 19

Fig. 19. Injection of *Ci-AP2L2* MO and *Ci-SoxB1* MO did not affect the expression of *Ci-cdc25* in animal blastomeres at the blastula stage. *Ci-cdc25* expression in the precursor blastomeres of ectoderm was examined by *in situ* hybridization. The expression of *Ci-cdc25* was not significantly affected in the embryos injected with hese MOs. Bar, 50 μm.

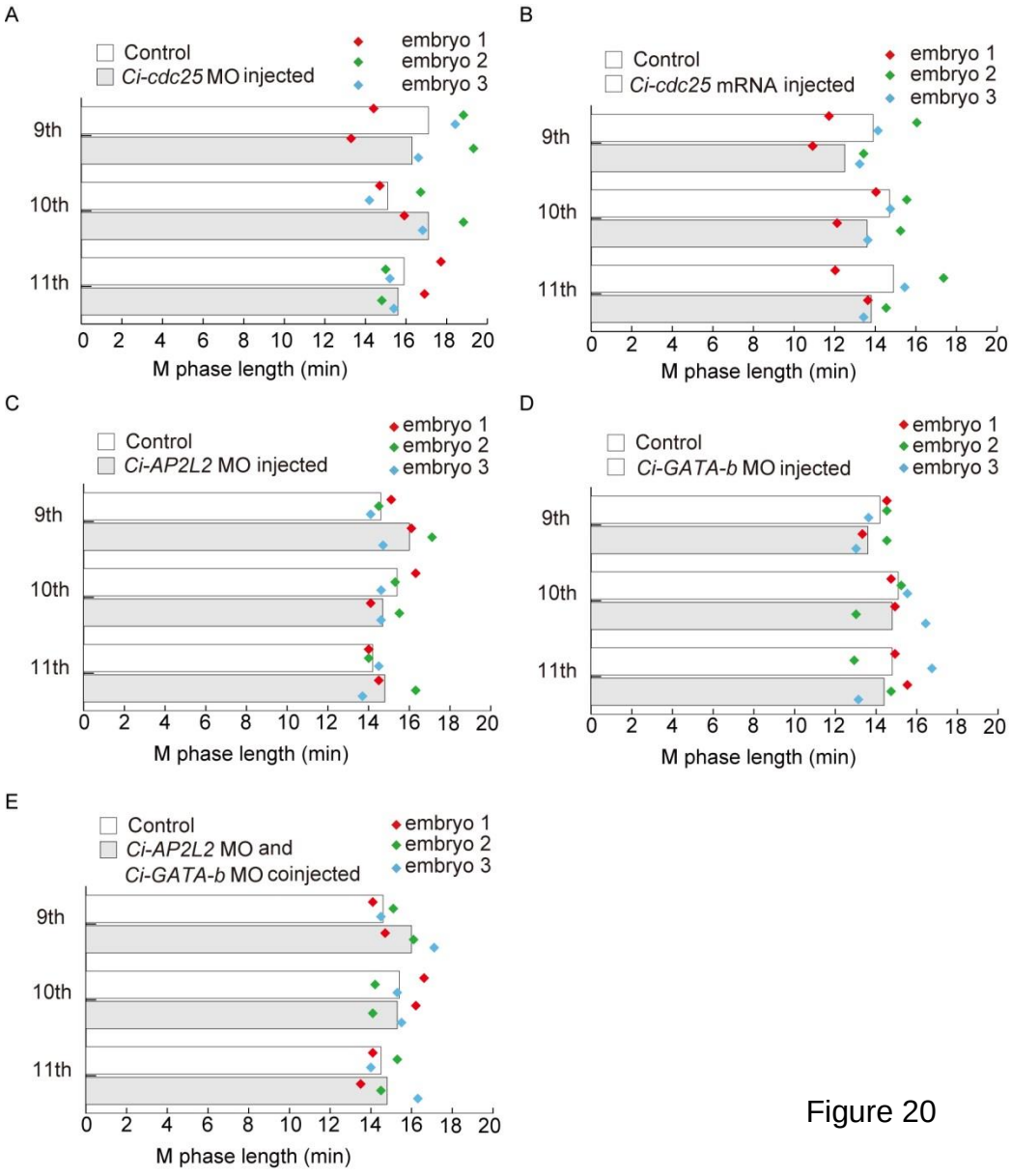
A
Control
Ci-cdc25 MO injected
embryo 1
embryo 2
embryo 3
9th
10th
11th
0 2 4 6 8 10 12 14 16 18 20
M phase length (min)
B
Control
Ci-cdc25 mRNA injected
embryo 1
embryo 2
embryo 3
9th
10th
11th
0 2 4 6 8 10 12 14 16 18 20
M phase length (min)
C
Control
Ci-AP2L2 MO injected
embryo 1
embryo 2
embryo 3
9th
10th
11th
0 2 4 6 8 10 12 14 16 18 20
M phase length (min)
D
Control
Ci-GATA-b MO injected
embryo 1
embryo 2
embryo 3
9th
10th
11th
0 2 4 6 8 10 12 14 16 18 20
M phase length (min)
E
Control
Ci-AP2L2 MO and
Ci-GATA-b MO coinjected
embryo 1
embryo 2
embryo 3
9th
10th
11th
0 2 4 6 8 10 12 14 16 18 20
M phase length (min)

Figure 20

Fig. 20. Effects of injecting *Ci-cdc25* MO, *Ci-cdc25* mRNA, *Ci-AP2L2* MO and *Ci-GATA-b* MO on the M-phase length of epidermal cells. (A-E) Interphase and mitosis was defined by nuclear localization of mVenus-PCNA fluorescence and its dispersal, respectively. Average M-phase length of epidermal cells at the 9th, 10th and 11th cell cycles (bar) and individual interphase length of three independent embryos (dots) are shown. The embryos 1, 2 and 3 corresponds the individuals given in the Fig. 3 and Fig. 12.